Geomorphology of the oceans

4 authors, including:

Peter Townsend Harris
GRID-Arendal
277 PUBLICATIONS   **7,882** CITATIONS

Elaine Baker
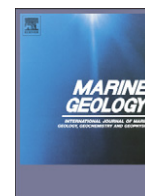The University of Sydney
68 PUBLICATIONS   **1,718** CITATIONS

Some of the authors of this publication are also working on these related projects:

Project   Ecological Marine Units (EMUs) View project

Project   Pacific Deep Sea Minerals and Mining View project

Geomorphology of the oceans

P.T. Harris [a,*], M. Macmillan-Lawler [b], J. Rupp [c], E.K. Baker [d]

[a] Geoscience Australia, Environmental Geoscience Division, GPO Box 378, Canberra, ACT 2601, Australia
[b] GRID-Arendal, Postboks 183, N-4802 Arendal, Norway
[c] Conservation International, 2011 Crystal Drive, Suite 500, Arlington, VA 22202, USA
[d] GRID-Arendal, c/o The University of Sydney, Sydney, NSW 2006, Australia

ARTICLE INFO

ABSTRACT

We present the first digital seafloor geomorphic features map (GSFM) of the global ocean. The GSFM includes 131,192 separate polygons in 29 geomorphic feature categories, used here to assess differences between passive and active continental margins as well as between 8 major ocean regions (the Arctic, Indian, North Atlantic, North Pacific, South Atlantic, South Pacific and the Southern Oceans and the Mediterranean and Black Seas). The GSFM provides quantitative assessments of differences between passive and active margins: continental shelf width of passive margins (88 km) is nearly three times that of active margins (31 km); the average width of active slopes (36 km) is less than the average width of passive margin slopes (46 km); active margin slopes contain an area of 3.4 million km^2 where the gradient exceeds 5°, compared with 1.3 million km^2 on passive margin slopes; the continental rise covers 27 million km^2 adjacent to passive margins and less than 2.3 million km^2 adjacent to active margins. Examples of specific applications of the GSFM are presented to show that: 1) larger rift valley segments are generally associated with slow-spreading rates and smaller rift valley segments are associated with fast spreading; 2) polar submarine canyons are twice the average size of non-polar canyons and abyssal polar regions exhibit lower seafloor roughness than non-polar regions, expressed as spatially extensive fan, rise and abyssal plain sediment deposits — all of which are attributed here to the effects of continental glaciations; and 3) recognition of seamounts as a separate category of feature from ridges results in a lower estimate of seamount number compared with estimates of previous workers.

Crown Copyright © 2014 Published by Elsevier B.V. All rights reserved.

1. Introduction

The publication of the first comprehensive, global map of seafloor physiography by Heezen and Tharp (1977) provided a pseudo-three-dimensional image of the oceans that has influenced generations of marine geoscientists. That image has been refined in recent years by the ETOPO bathymetric grids (Smith and Sandwell, 1997) that, along with other similar products (Becker et al., 2009), have provided the bases for quantitative analyses of the global distribution of specific seafloor features. Examples include studies of seamounts (Kitchingman and Lai, 2004; Etnoyer et al., 2010; Yesson et al., 2011), submarine canyons (Harris and Whiteway, 2011) and mid-ocean ridges (Baker and German, 2004). Although we now have better bathymetric datasets than ever before, there had been little effort to interpret these data to create an updated, comprehensive map of seabed physiography prior to the present study. Currently, the best available global seafloor geomorphic features map is over 30 years old (Agapova et al., 1979).

To address this knowledge gap, a new digital, global seafloor geomorphic features map (GSFM) has been created using a combination of manual and ArcGIS methods based on the analysis and interpretation of a modified version of the SRTM30_PLUS global bathymetry grid (Becker et al., 2009; Fig. 1). The new map includes global spatial data layers for 29 categories of geomorphic features, defined by the International Hydrographic Organisation and other sources (Table 1). The GSFM provides the basis for the first global estimates of physiographic statistics (area, number, mean size, etc.) for terraces, basins, plateaus, abyssal ridges, rift valley segments, glacial troughs, escarpments, sills, trenches, troughs, fans and bridges.

2. Overview of materials, methods and error analysis

2.1. Materials and methods

The GSFM is based on interpretation of the Shuttle Radar Topography Mapping (SRTM30_PLUS) 30-arc second database (Becker et al., 2009). SRTM30_PLUS data were supplemented in two areas, around Australia (Whiteway, 2009) and on the European continental shelf (EMODNet, 2013), with additional data sources (Fig. 1). In all cases the data were reduced to a uniform grid spacing of 30 arc sec (~1 km)

* Corresponding author.
E-mail address: peter.harris@ga.gov.au (P.T. Harris).
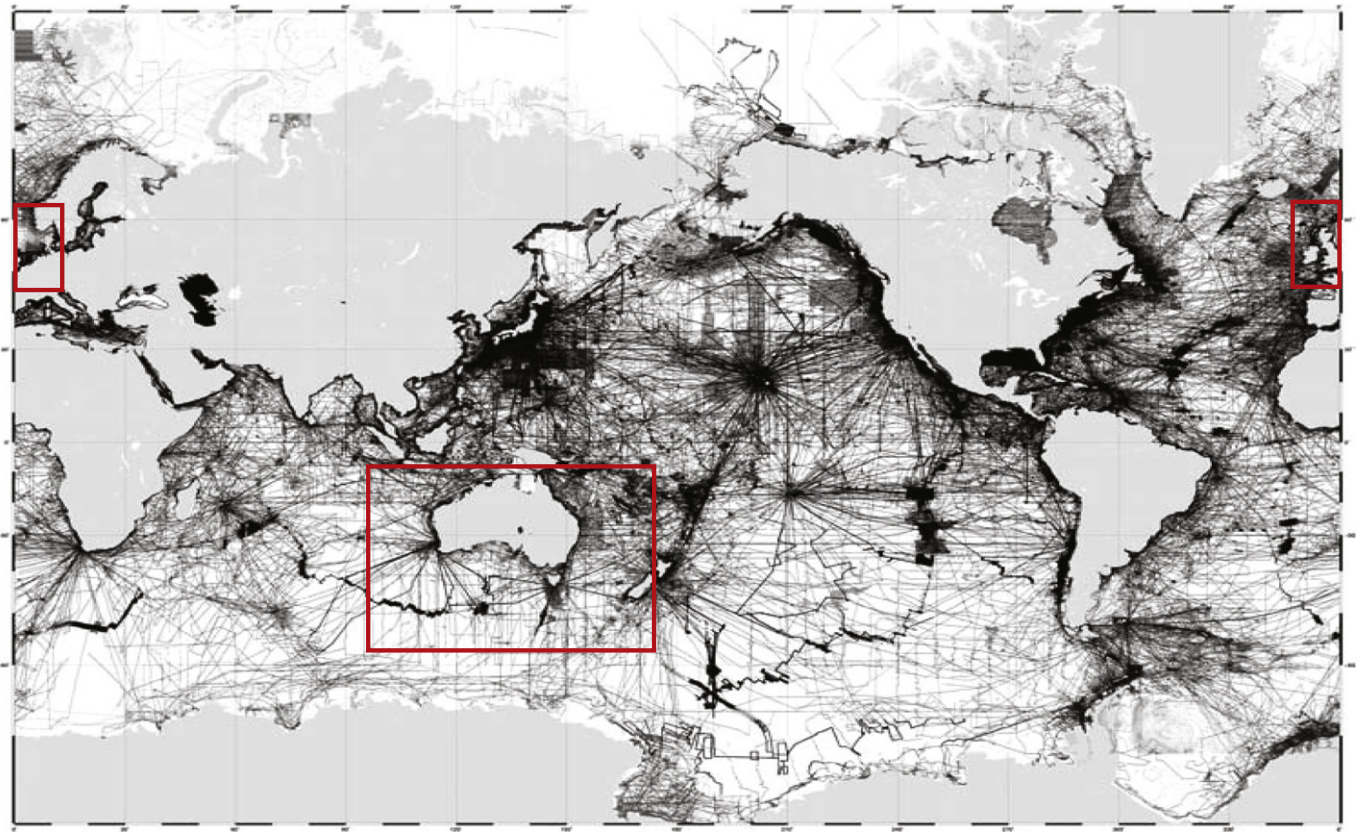
Fig. 1. Ship track plots of all the soundings used in the SRTM30 PLUS global bathymetry grid (Becker et al., 2009). Red boxes indicate areas where the Australian bathymetric model (Whiteway, 2009) and the EMODNet (2013) data were used to supplement the SRTM30_PLUS data.

to ensure consistency in the interpretation of the data. Interpretation of geomorphic features was based on contoured data, false colour shaded relief, analysis of slope and other tools from ArcGIS as described in detail below for each of the geomorphic feature types.

The output of this project is a series of ArcGIS data layers; we will refer throughout this report to geomorphic feature "data layers", as defined by ArcGIS. Features were mapped using one or more of three generalised methods: 1) manual digitisation; 2) algorithm-assisted manual digitisation; and 3) algorithm digitisation with visual check. Details of the approach taken for each layer are outlined in the following sections.

Manual digitisation and algorithm-assisted digitisation were carried out at a spatial scale of 1:500,000 (unless otherwise indicated), guided mainly by bathymetric contours at 10 m intervals (continental shelf), 50 m intervals (Antarctic continental shelf) and 100 m intervals (all other ocean areas). The selection of these contour intervals is based on the vertical resolution of the SRTM30_PLUS, which is ~100 m in deep sea areas where satellite altimeter data are used. The SRTM30_PLUS bathymetry is based on a new satellite-gravity model where the gravity-to-topography ratio is calibrated using 298 million edited soundings, which come from a number of different sources (see Becker et al., 2009, for details). The existing satellite gravity model (Smith and Sandwell, 1997) is then fitted to the edited sounding dataset to produce the SRTM30_PLUS grid. The satellite gravity model extends only to 80° latitude, so the Arctic Ocean bathymetric model of Jakobsson et al. (2008) is incorporated into the SRTM30_PLUS grid.

The resolution of the data underlying the grid varies depending on the available sounding data (Fig. 1). Becker et al. (2009) state that about 10% of the 600 million 1 km grid cells in the SRTM30_PLUS grid are constrained by one or more soundings. If the grid size is increased to 2 km then about 24% of the cells are constrained by one or more soundings. Smith and Sandwell (1997) state that in the worst

case scenario (i.e. where there are no soundings) the lowest resolution of the satellite gravity data is around 12.5 km.

The bathymetric contours were supplemented by other representations of the bathymetry data, such as shaded relief maps and false colour gradient (slope) maps and also using available Supplementary information including global sediment thickness (Divins, 2003), ocean crust age (Müller et al., 1997), the global geomorphic features map of Agapova et al. (1979), a seafloor geomorphology map of Australia (Heap and Harris, 2008) and the GEBCO Gazetteer of Undersea Feature Names (IHO-IOC, 2012).

2.2. Error analysis

The error associated with area estimations for each feature derives from several sources, including the spatial distribution and accuracy of depth measurements used in creating the bathymetric model (Fig. 1), errors within the supporting data sources used in making the classification (cited above), errors derived from smoothing of polygons, and errors associated with the misclassification of features. Given the grid resolution of the SRTM30_PLUS bathymetric model is 30 arc sec, or approximately 1 km, the location of the derived feature boundaries will reflect this resolution. Assuming a precision of interpretation of the bathymetric model is 3×3 grid cells in any dimension, we have rounded all area estimations to the nearest 10 km^2.

In order to investigate the potential sources of error derived from misclassification, selected features from this study were compared to existing global scale datasets. The seamount feature layer was checked against the seamount layer of Yesson et al. (2011). Both these data layers were derived from versions of the SRTM30_PLUS bathymetric model. Yesson et al. (2011) identified a total of 33,452 seamounts and guyots (features > 1000 m elevation) whilst this study, using a more

Table 1

Hierarchy of geomorphic features mapped in the present study. Mutually exclusive base layer features are the shelf, slope, abyss and hadal zones. Classification layers were produced for the shelf (low, medium and high profile) and abyssal layers (plains, hills and mountains), based on an analysis of vertical relief as described in the text. The occurrence of some features is confined to one of the base layers, whereas the occurrence of other features is confined to two or more base layers, as illustrated by shading; elsewhere the feature layers and classification layers may overlay each other (e.g. escarpments on seamounts; ridges and seamounts on abyssal mountains; etc.). Basins and sills are the only features that occur over all four base layers. *The coral reefs layer was obtained from the Reefs at Risk Revisited database (WRI, 2011). It was not modified in any way and is included here for convenience and reference purposes. **Includes: a) major ocean basins (abyssal and hadal zones); b) large basins of seas and oceans (large to moderate size, abyssal and hadal zones); c) small basins of seas and oceans (small size, abyssal and hadal zones); d) basins (small to moderate size) perched on the continental slope; and e) basins (small to moderate size) perched on the continental shelf.

1. Shelf	2. Slope	3. Abyssal	4. Hadal
5. Low relief <10 m	10. Terraces	11. Abyssal plains (<300 m relief)	
6. Medium relief 10–50 m		12. Abyssal hills (300–1,000 m relief)	
7. High relief >50 m		13. Abyssal mountains (>1,000 m relief)	
8. Shelf valleys		14. Continental rise	
9. Glacial troughs		15. Mid–ocean ridge	
Coral reefs*		16. Rift valley	
17. Basins** (shelf perched)	17. Basins** (slope perched)	17. Basins**	17. Basins**
18. Sills	18. Sills	18. Sills	18. Sills
	19. Escarpments	19. Escarpments	19. Escarpments
	20. Seamounts	20. Seamounts	20. Seamounts
	21. Guyots	21. Guyots	
	22. Canyons (shelf incising)	22. Canyons (shelf incising)	
	23. Canyons (blind)	23. Canyons (blind)	
	24. Ridges	24. Ridges	24. Ridges
	25. Troughs	25. Troughs	25. Troughs
		26. Trenches	26. Trenches
		27. Bridges	27. Bridges
	28. Fans	28. Fans	
	29. Plateaus	29. Plateaus	

strict definition for seamounts of conical form (thus excluding ridge-shaped features), identified 9951 seamounts and a further 283 guyots for a total of 10,234 comparable features (see Sections 5.10 and 5.11 below for details). Eighty nine percent of the seamounts and guyots identified in this study were also identified by Yesson et al. (2011). Conversely, only around 45% of the Yesson et al. (2011) seamounts were identified in this study as either seamounts or guyots. However, a further 32% of the Yesson et al. (2011) seamounts coincided with ridge features identified in this study. Yesson et al. (2011) acknowledged that their method may overestimate seamount numbers along ridges and in areas where faulting and seafloor spreading creates highly complex topography. It should also be noted that many features identified as individual seamounts by Yesson et al. (2011) were classed as multiple peaks on a single ridge in this study.

Another study of seamount basal area published by Etnoyer et al. (2010) provides a further dataset for comparison. These workers estimated seamount basal area from the satellite-derived (Smith and Sandwell, 1997) vertical gravity gradient, assuming a circular cross section and using an available inventory of 11,880 seamount locations. The estimated global seamount basal area of 10,079,658 km^2 (Etnoyer et al., 2010) is comparable to the figure estimated in this study for combined seamounts and guyots (8,796,150 km^2), which was also restricted to seamounts of conical form (Table 1). Further, the average seamount sizes are also comparable for the two studies (848 km^2 and 860 km^2, respectively).

Submarine canyons were checked against the dataset of Harris and Whiteway (2011). The Harris and Whiteway (2011) dataset was developed using the ETOPO2 bathymetric grid which is at a coarser resolution than the SRTM 30_PLUS dataset used in this study. Eighty point five percent of the Harris and Whiteway (2011) large submarine canyons were identified in this study. We identified a large number of additional canyons, with over 50% of the canyons identified in this study not

included in the Harris and Whiteway (2011) dataset. Our additional canyons may be a result of the improved data resolution used in this study and the fact that the Harris and Whiteway (2011) study was limited to the continental margin, whilst this study also identified canyons on plateaus attached to the continental margin.

The final comparison of classification accuracy examined the proximity of active mid-ocean ridge hydrothermal vents with the rift valley/spreading ridge features. The proximity of active hydrothermal vents from the InterRidge vents database ver 3.2 (Beaulieu, 2013) was examined in relation to the rift valley/spreading ridge layers from this study. There was a strong correlation between the two data sources with 87.7% of known and predicted hydrothermal vents contained within the rift valley/spreading ridge features.

2.3. Approach to presentation of methods and results

The data in this paper are presented for major ocean regions, using the boundaries modified from 'The Limits of Oceans and Seas' (IHO, 1953) to include only major oceans and marginal seas and to include the Southern Ocean south of 60°S. This gives 8 ocean regions as follows: the Arctic, Indian, North Atlantic, North Pacific, South Atlantic, South Pacific and the Southern Oceans and the Mediterranean and Black Seas (Fig. 2). In the following sections the methods used to map separate features are described. Furthermore, the initial results for each feature giving the mapped area and feature enumeration are available as Supplementary tables containing statistics for each of the 8 major ocean regions and for the global ocean. In the final results section the integrated map is presented and the defining characteristics of each ocean region are summarized.

3. Base feature interpretation methods and initial results

The geomorphology of the seafloor is viewed in this study as a hierarchy of *base layers* for the shelf, slope, abyss and hadal zones, overlain by *classification layers* and discrete *feature layers* (Table 1). Two of the base layers (shelf and abyssal) are subdivided into *classification layers* based on roughness: low, medium and high relief shelves (layers 5, 6 and 7; Table 1); and abyssal plains, abyssal hills and abyssal mountains (layers 13, 14 and 15; Table 1; see below for detailed descriptions). Whereas the four base layers are mutually exclusive, the classification layers and feature layers may overlay each other as illustrated in Table 1.

3.1. Base feature 1. Continental shelf (Supplementary Table 1)

The continental shelf is defined by IHO (2008) as "a zone adjacent to a continent (or around an island) and extending from the low water line to a depth at which there is usually a marked increase of slope towards oceanic depths". The low-water mark is taken in this study as the 0 m depth contour. The shelf break (i.e. the line along which there is marked increase of slope at the seaward margin of a shelf) was digitised manually at a nominal spatial scale of 1:500,000 in ArcGIS based on 10 m, 50 m and 100 m contours, depending on the slope and bathymetric profile of the region. In most cases 100 m contours were sufficient at the selected scale of 1:500,000 to identify the shelf break. However, where there was a gradual break in slope over a broad area, more closely spaced contours were used. Floating ice shelves cover large sections of the Antarctic continental shelf and these areas were simply left blank. This is the case, for example, at one area located at 70° south latitude and 1° west longitude, where a floating ice shelf covers the shelf and there is a noticeable gap in the shelf and slope classifications along the margin.
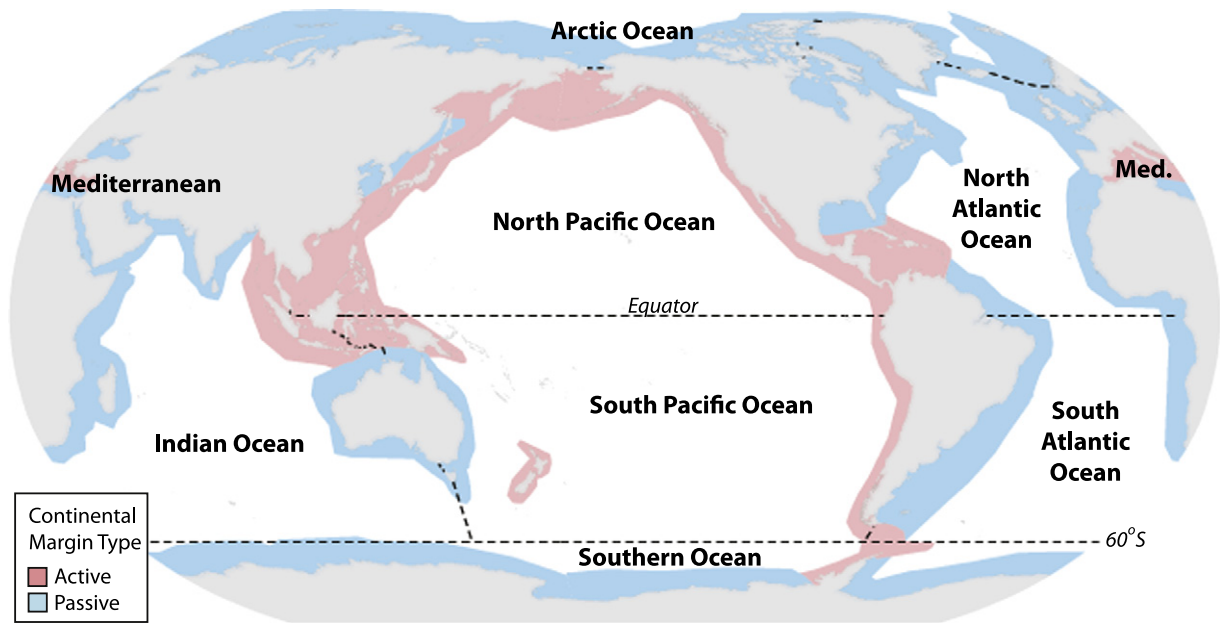
Fig. 2. Map showing the locations of active and passive continental margins and the eight ocean regions described in the text.

3.2. Base feature 2. Continental slope (Supplementary Table 1)

The slope is "the deepening sea floor out from the shelf edge to the upper limit of the continental rise, or the point where there is a general decrease in steepness" (IHO, 2008). In this study, the foot of slope was digitised manually at a nominal spatial scale of 1:500,000 in ArcGIS based on 100 m contours and 3D viewing. ArcGIS was used to highlight zones of abrupt changes in seabed gradient (contour spacing) which suggests the foot of slope in many areas. In areas where marginal plateaus abut the margin, the foot of slope was allowed to extend offshore to encompass the plateau feature, where a clear seaward dipping gradient was apparent. Otherwise the first significant decrease in gradient encountered in a seaward direction from the shelf break was selected as the foot of slope. Note our foot of slope locations are based only on bathymetric data and our interpretation is not intended to define the foot of slope under Article 76 of the 1982 United Nations Convention on the Law of the Sea, particularly in areas of geomorphologically complex, continent–ocean transition.

3.3. Base feature 3. Abyss (Supplementary Table 1)

The abyss is the area of seafloor located at depths below the foot of the continental slope and above the depth of the hadal zone (defined as deeper than 6000 m). The abyss feature layer was created by clipping a layer representing the ocean with the shelf, slope and hadal layers. The abyssal layer is sub-divided into three categories based on roughness (see Section 4.2 for details).

3.4. Base feature 4. Hadal (Supplementary Table 1)

The hadal zone is defined in this study as seafloor occurring at depths of >6000 m (based on the SRTM bathymetry grid). A majority filter (ArcGIS 10 → Spatial Analyst → Generalisation → Majority Filter, Number of neighbours = 8, Replacement threshold = half) was run twice over to remove small-scale pixilation in the classified grid. The classified grid was converted to a vector layer. Polygons with an area of <100 km^2 were deleted and similarly holes of <100 km^2 were filled. Finally, the resulting vector layer was smoothed (ArcGIS 10 → Cartography Tools → Generalisation → Smooth Polygon, Smoothing Algorithm = PAEK, Smoothing tolerance = 2 nautical miles).

4. Classification layer methods and initial results

4.1. Continental shelf relief classes (Supplementary Table 2)

A classification of the continental shelf based on vertical relief yielded three classes: Low-relief shelf; Medium-relief shelf; and High-relief shelf. To generate these classes, the SRTM model was sub-classified based on the variation over a five-cell radius (80 cells) into areas of low (<10 m), medium (10–50 m) and high (>50 m) vertical relief. The first step involved masking the SRTM model with the shelf layer followed by the calculation of focal statistics (ArcGIS → Spatial Analyst Tools → Neighbourhood → Focal statistics, Neighbourhood = circle, radius = 5, Statistic type = STD). The STD raster was classified into three standard deviation categories of <2.5, 2.5–12.5, and >12.5. The classified raster was converted to a vector layer, and the resulting vector layer was smoothed (ArcGIS 10 → Cartography Tools → Generalisation → Smooth Polygon, Smoothing Algorithm = PAEK, Smoothing tolerance = 2 nautical miles). The area of the individual feature polygons was calculated and features of <100 km^2 were merged into the largest adjacent polygon.

4.2. Abyssal classification layers (Supplementary Table 3)

The SRTM model was classified based on the variation over a 25 cell radius (1976 cells) into areas of low, medium and high relief, broadly corresponding to abyssal plains (<300 m relief), abyssal hills (300–1000 m relief) and abyssal mountains (>1000 m relief). The first step involved masking the SRTM30_PLUS model with the abyss layer, and then applying focal statistics in ArcGIS (ArcGIS → Spatial Analyst Tools → Neighbourhood → Focal statistics, Neighbourhood = circle, radius = 25, Statistic type = STD). The STD raster was classified into three standard deviation categories of <75 m, 75–250, and >250. The classified raster was converted to a vector layer. The resulting vector layer was smoothed (ArcGIS 10 → Cartography Tools → Generalisation → Smooth Polygon, Smoothing Algorithm = PAEK, Smoothing tolerance = 2 nautical miles). The area of the individual feature polygons was calculated and features of <100 km^2 were merged into the largest adjacent polygon.

5. Discrete feature layer methods and initial results

Feature types appearing in the upper section of Table 1 (without shading) refer to features that overlay only one base layer. For example, shelf valleys are found only on the continental shelf base layer, and the continental rise, spreading ridges and rift valleys are found only on the abyssal base layer. All other feature types are found overlaying more than one base layer as indicated by the shaded feature type names (Table 1). Feature types are as defined by the International Hydrographic Organisation (IHO, 2008) unless specified otherwise below. In every case, the GEBCO Gazetteer of geographic names of undersea features (IHO-IOC, 2012) was used to ensure all named features were assessed for inclusion in our map. Although most features were included within their indicated category, there were several features named in the GEBCO Gazetteer for which there was no evidence of the feature's existence or in some cases the named feature was included in a different, more appropriate category.

5.1. Shelf valleys (Supplementary Table 4)

Valleys incised more than 10 m into the continental shelf were digitised by hand. To qualify for inclusion in this study, shelf valleys had to be greater than 10 km in length and >10 m in depth overall. Only features that had a definite elongated shape were included as valleys, nominally more than 4 times greater in length than width. Features that intersected the shelf break and extended both onto the shelf and down-slope (where they become submarine canyons) were also included. Shelf valleys are most common in polar areas where valleys have formed by glacial erosion (Hambrey, 1994; Anderson, 1999). Non-glacial shelf valleys were formed mainly during the Pleistocene ice ages by fluvial erosion when rivers flowed across what is now the submerged continental shelf, and also by the erosive effects of tidal and other ocean currents. Other non-glacial shelf valleys have formed in some tropical carbonate provinces, where valleys appear as inter-reef channels formed when sea level changes have left submerged banks (drowned reefs) stranded offshore (Harris et al., 2005).

5.2. Glacial troughs (Supplementary Table 5)

Shelf valleys at high latitudes incised by glacial erosion during the Pleistocene ice ages form elongated troughs, typically trending across the continental shelf and extending inland as fjord complexes (Hambrey, 1994). The largest of these features are glacial troughs, characterised by depths of over 100 m (often exceeding 1000 m depth) and are distinguished from shelf valleys by an over-deepened longitudinal profile that reaches a maximum depth inboard of the shelf break, thus creating a perched basin on the shelf with an associated sill (Hambrey, 1994). Glacial troughs were digitised by hand based on 50 m contoured data for the Antarctic and 10 m contoured data for other shelf areas.

5.3. Terraces on the continental slope (Supplementary Table 6)

Terraces are "an isolated (or group of) relatively flat horizontal or gently inclined surface(s), sometimes long and narrow, which is (are) bounded by a steeper ascending slope on one side and by a steeper descending slope on the opposite side" (IHO, 2008). In this study terraces (broad steps) were calculated based on the gradient of the SRTM30_PLUS model. The SRTM30_PLUS model was masked using the slope feature layer (i.e. terraces we only mapped on the continental slope). The gradient of the masked SRTM30_PLUS model was then calculated. The resulting grid was classified into two gradient classes, greater than 1° and less than 1°. A majority filter (ArcGIS 10 → Spatial Analyst → Generalisation → Majority Filter, Number of neighbours = 8, Replacement threshold = half) was run twice over to remove small sized pixilation in the classified grid. The cells

with a value of less than 1° of gradient were then converted to a vector layer, smoothed (ArcGIS 10 → Cartography Tools → Generalisation → Smooth Polygon, Smoothing Algorithm = PAEK, Smoothing tolerance = 10 nautical miles) and polygons of <100 km² filtered out. The polygons were then overlaid with the 100 m contours and adjusted to remove artefacts from the processing and to better capture the shape of the terraces.

A total of 1230 terraces were identified in this study, covering an area of 2,303,490 km², equal to 0.64% of the oceans and 11.6% of the area of the continental slope. Terraces are most common on the continental slopes of the Arctic and Indian Oceans, where they characterise over 21% of the continental slope. Terraces occupy less than 6% of the slope in the Mediterranean and Black Seas, the North Pacific and the South Pacific Oceans. The largest terrace is on the North West Shelf of Australia, which covers an area of 104,470 km².

5.4. Continental rise (Supplementary Table 7)

The continental rise was digitised by hand at a nominal spatial scale of 1:3,000,000 in ArcGIS based on 100 m contours. A map of global ocean sediment thickness (Divins, 2003) was used to assist with identifying potential rise areas. In general the rise was confined to areas of sediment thickness of >300 m.

Criteria for identification of continental rises included the occurrence of a smooth sloping seabed as indicated by evenly-spaced, slope-parallel contours (Curray et al., 2002; Dowdeswell et al., 2008; Covault, 2011). In this study, the term "Rise" was restricted to features that abut continental margins and does not include the mid-ocean ridge (or "rise"), which was mapped as a separate feature. The GEBCO Gazetteer of geographic names of undersea features (IHO-IOC, 2012) was used to ensure all named features were included. There is considerable variability in the mean thickness of sediment characterising rises in the different ocean regions, ranging from around 450 m in the South Pacific to over 3100 m in the Indian Ocean.

5.5. Mid-ocean spreading ridges (Supplementary Table 8)

Mid-ocean spreading ridges are "the linked major mid-oceanic mountain systems of global extent" (IHO, 2008). Spreading ridges are distinguished from other ridges in this study (see definition of ridges below). They were mapped by hand based on their appearance as ridge-like features that coincide with the youngest ocean crust as mapped by Müller et al. (1997) in their "EarthByte" digital age grid of the ocean floor. Spreading ridges that were not visible in the SRTM30_PLUS bathymetry (100 m contours) were not included in our interpretation, but there is otherwise no vertical size limitation on spreading ridges (they overlay the abyssal plains, hills or mountains classification layers in different locations). The mid-ocean spreading ridge covers the largest fraction of abyssal zone in the Arctic Ocean, where it characterises 4.76% of the area of abyssal zone, and it is absent from the Mediterranean and Black Sea. The greatest area of mid-ocean ridges occurs in the South Pacific Ocean where this feature type covers an area of 1,868,490 km².

5.6. Rift valleys (Supplementary Table 9)

Rift valleys were mapped as separate features in the present study where they are clearly evident in SRTM30_PLUS bathymetric data. Rift valleys are confined to the central axis of mid-ocean spreading ridges; they are elongated, local depressions flanked generally on both sides by ridges (Macdonald, 2001). They were mapped by hand based on 100 m contours. Rift valleys cover the largest fraction of abyssal zone in the Arctic Ocean, where they characterise 0.622% of that area. The greatest area of rift valleys occurs in the Indian Ocean where they cover 165,220 km².
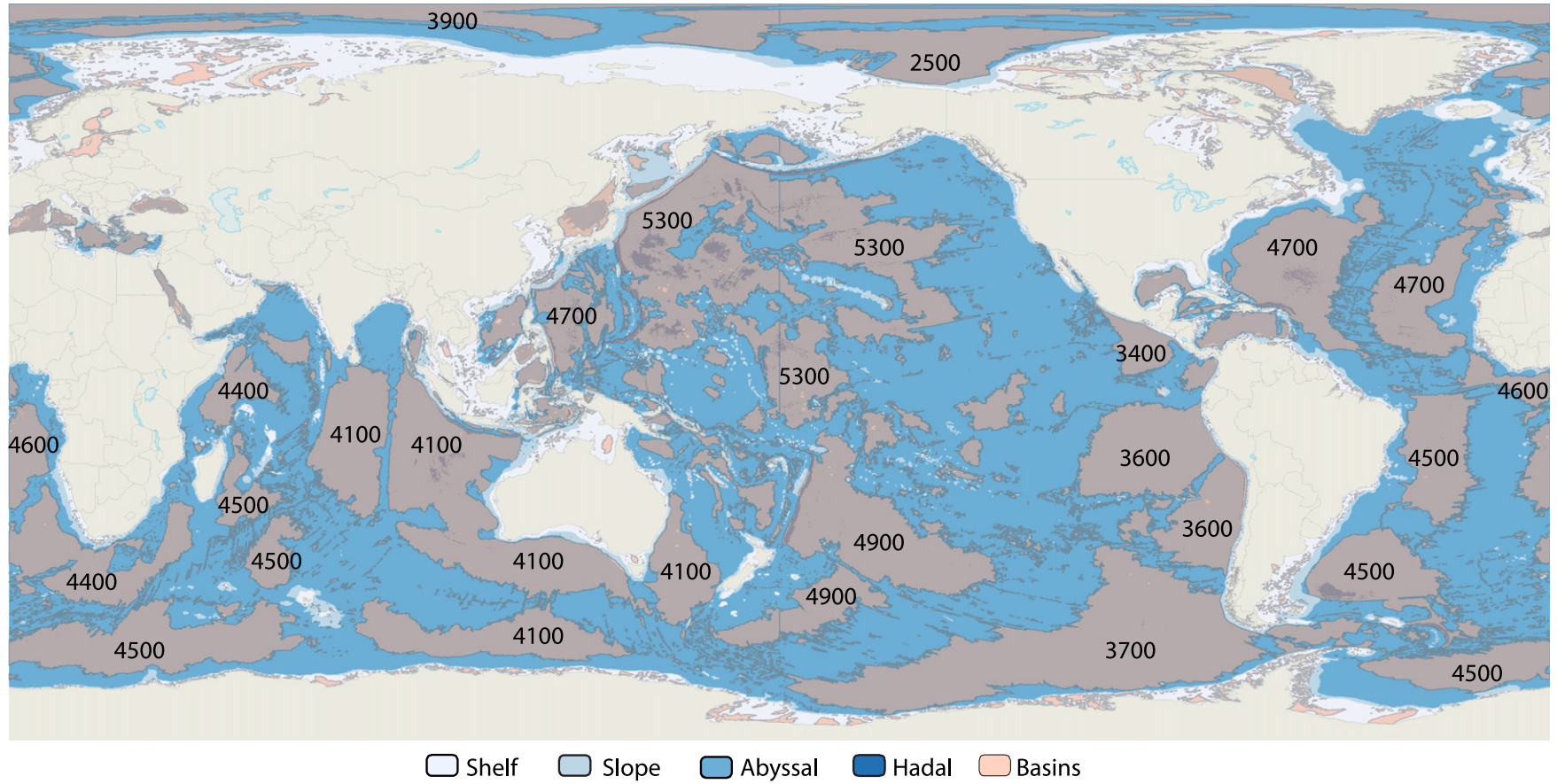
Fig. 3. Basins mapped in this study. The numbers indicate contour depths of major ocean basins based on the most shallow, closed, bathymetric contour that defines the basin outline, illustrating that the deepest basins are located in the northwest Pacific.

5.7. Basins (Supplementary Table 10)

Basins are "a depression, in the sea floor, more or less equidimensional in plan and of variable extent" (IHO, 2008). In this study basins are restricted to seafloor depressions that are defined by closed bathymetric contours. Basins were mapped based on the identification of the most shoal, closed, bathymetric contours, examined regionally for the major ocean basins and shelf seas. Basins of the major oceans are nominally bounded by the foot of slope and by the mid-ocean spreading ridges (Wright and Rothery, 1998; Gille et al., 2004). However, numerous smaller basins of the bathyal and hadal zones, located outside of the major ocean basin areas, were mapped separately, again by identification of the most shoal, closed, 100 m, bathymetric contours. At abyssal depths we distinguish between major ocean basins, which are large basins (>800 km^2), and small basins (<800 km^2). The depths of major ocean basins (defined by the most shoal closed contour that they contain) illustrate that the major ocean basins in the Northwest Pacific are the deepest, at 5300 m (Fig. 3).

We also identified basins perched on the slope, again mapped by identification of the most shoal, closed, 100 m, bathymetric contours that defined a discrete basin. Basins perched on the Antarctic shelf were mapped by identification of the most shoal, closed, 50 m, bathymetric contours that defined a discrete basin. Basins perched on the rest of the world's shelf areas were mapped by identification of the most shoal, closed, 10 m, bathymetric contours that defined a discrete basin. These included the basins within shelf seas, glacial troughs and fjord basins found in the higher latitudes. A key point about basins is that they overlay not only the basal layers, but also other features (i.e.

other individual features may occur partly or wholly within a basin or basins). Basins cover the greatest area across all feature layers, equal to 158,529,660 km^2, or 43.8% of the oceans.

5.8. Sills (Supplementary Table 11)

Sills are "a sea floor barrier of relatively shallow depth restricting water movement between basins" (IHO, 2008). Thus every basin has a sill, over which fluid would escape if the basin were filled to overflowing. The identification of sills in this study is based on selecting contours at a specified interval of 10 m (shelf except for Antarctica), 50 m (Antarctic shelf) or 100 m (all other areas) depending upon the location. Selecting the most shoal, closed contour defines the basin; one contour interval above this typically identifies a discrete location where contours "escape" from the basin and join into the regional bathymetry. This location is mapped as the sill. Sills were mapped for all of the major ocean basins (Fig. 3) and seas and for the larger basins perched on the continental shelf; sills were not mapped for the smaller basins perched on the slope or shelf or for the smaller abyssal basins.

5.9. Escarpments (Supplementary Table 12)

Escarpments are "an elongated, characteristically linear, steep slope separating horizontal or gently sloping sectors of the sea floor in non-shelf areas. Also abbreviated to scarp" (IHO, 2008). Escarpments, like basins, overlay other features (i.e. other individual features may be partly or wholly covered by escarpments). Thus features like the continental slope, seamounts, guyots, ridges and
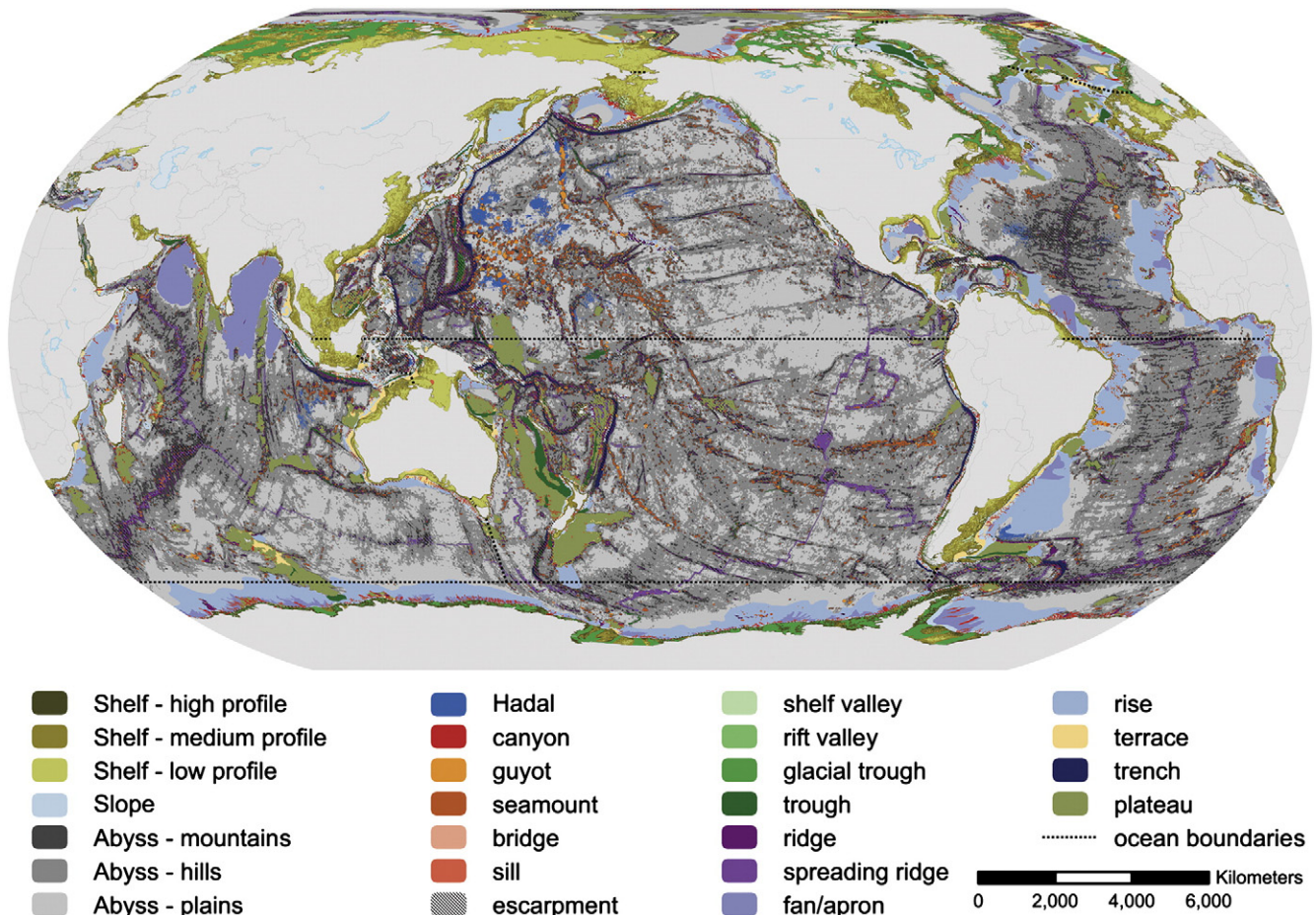

Fig. 4. Geomorphic features map of the world's oceans. Dotted black lines mark boundaries between major ocean regions. Basins are not shown.

Table 2
Statistics on the width of the geomorphic continental shelf, measured by finding the nearest point of land from the shelf break at 0.1° (~10 km) intervals. The continental shelf has an average width of 57 ± 0.41 km, and the average width along passive continental margins (84 ± 0.66 km) is more than twice that of active margins (31 ± 0.4 km).

Shelf	Active margins		Passive margins		All margins	
Ocean	Mean (km)	Maximum (km)	Mean (km)	Maximum (km)	Mean (km)	Maximum (km)
Arctic Ocean	0	0	104.1 ± 1.7	389	104 ± 1.72	389
Indian Ocean	19 ± 0.61	175	47.6 ± 0.8	238	37 ± 0.58	238
Mediterranean and Black Seas	11 ± 0.29	79	38.7 ± 1.5	166	17 ± 0.44	166
North Atlantic Ocean	28 ± 1.08	259	115.7 ± 1.6	434	85 ± 1.14	434
North Pacific Ocean	39 ± 0.71	412	34.9 ± 1.2	114	39 ± 0.68	412
South Atlantic Ocean	24 ± 2.6	55	123.0 ± 2.5	453	104 ± 2.4	453
South Pacific Ocean	21 ± 0.4	136	49.6 ± 1.9	207	24 ± 0.42	207
Southern Ocean	214 ± 2.86	357	96.1 ± 2.0	778	110 ± 1.92	778
All oceans	31 ± 0.4	412	88.2 ± 0.7	778	57 ± 0.41	778

submarine canyons (for example) may be sub-classified in terms of their area of overlain escarpment.

Escarpments were calculated based on the gradient of the SRTM30_PLUS model. Gradient was calculated (ArcGIS 10 → DEM Surface Tools (Jenness et al., 2012) → Slope, Slope computation method = 4-cell method) and classified into areas of gradient greater than 5° and less than or equal to 5°. A majority filter (ArcGIS 10 → Spatial Analyst → Generalisation → Majority Filter, Number of neighbours = 8, Replacement threshold = half) was run twice over to remove small sized pixilation in the classified grid. Areas of the filtered grid with gradient greater than 5° were converted to a vector layer. The area of the individual feature polygons was calculated and features of <100 km² were deleted; similarly holes in features smaller than 100 km² were filled. Finally, the resulting vector layer was smoothed (ArcGIS 10 → Cartography Tools → Generalisation → Smooth Polygon, Smoothing Algorithm = PAEK, Smoothing tolerance = 2 nautical miles). Thus, in summary, a seafloor gradient exceeding 5° over an area of >100 km², located in slope, abyssal and hadal zones, is classified here as an "escarpment".

5.10. Seamounts (Supplementary Table 13)

Seamounts are "a discrete (or group of) large isolated elevation(s), greater than 1000 m in relief above the sea floor, characteristically of conical form" (IHO, 2008). Seamounts are thus defined as peaks that rise over 1000 m above the seafloor, calculated based on the SRTM30_PLUS model. We adhered strictly to the requirement that seamounts are "of conical form", thus distinguishing "seamounts" (having a length/with ratio < 2) from ridges (having a length/width ratio ≥ 2). The criterion of a length/width ratio of <2 for seamounts is consistent with the geomorphic analysis of Mitchell (2001). Seamounts are, furthermore, distinguished from flat-topped guyots (see below).

There have been a number of previous studies published on probable locations of seamounts in the oceans, which have mainly focussed on identifying individual seamount peaks (Kitchingman and Lai, 2004). Global seamount basal area was also estimated by Etnoyer et al. (2010) and Yesson et al. (2011). We mapped the basal area of seamounts as well as summit morphology (i.e. distinguishing between ridges, guyots and seamounts) in order to produce a broad range of statistical measures of seamount geomorphology. A two-stage process was used to generate the seamount layer. The first stage involved only automated algorithms whereas the second stage involved manual checking and revision.

5.10.1. Stage 1

Peaks over 1000 m high were identified through two methods. The first method involved running 10 iterations of focal statistics (ArcGIS 10 → Spatial Analyst Tools → Neighbourhood → focal statistics, Neighbourhood = Annulus, radius = 5, 10, 15, 20, 25, 30, 35, 40, 45, 50, statistic type = MAXIMUM) to calculate the shallowest depth from a focal point at various scales. Each of the 10 focal statistic iterations was then subtracted from the original SRTM30_PLUS model and classified to identify all areas having >1000 m depth (height above the level of surrounding seafloor) difference. The classified grids were converted to vector layers, merged together and the mid-point of the resulting polygon calculated (ArcGIS 10 → Data Management Tools → Features → Feature to point). This method was ideal for classical, conical-shaped seamounts on flat ocean floor, although the method did miss some seamount peaks. Therefore, a second method was applied to identify additional peaks over 1000 m high, which involved inverting the SRTM30_PLUS model and then filling in the sink holes (ArcGIS → Spatial Analyst Tools → Hydrology → fill, no z limit). Where the difference between the filled grid and the original grid was greater than 1000 m, the centroids were again calculated, and these were also identified as potential seamounts. This second method identified many features that were not seamounts, such as plateaus, and as such was used to supplement the first method.

Table 3
Statistics on the width of the geomorphic continental slope, measured as the horizontal distance between the shelf break and foot of slope.

Slope	Active margins		Passive margins		All margins	
Ocean	Mean (km)	Maximum (km)	Mean (km)	Maximum (km)	Mean (km)	Maximum (km)
Arctic Ocean	0 ± 0	0.0	33 ± 0.5	287.3	33 ± 0.5	287.3
Indian Ocean	50.4 ± 0.9	205.3	52.4 ± 0.7	255.2	51.9 ± 0.6	255.2
Mediterranean and Black Seas	25.8 ± 0.5	118.0	47 ± 1.1	127.6	31 ± 0.5	127.6
North Atlantic Ocean	26.7 ± 0.5	144.2	63.6 ± 0.8	368.2	51.1 ± 0.6	368.2
North Pacific Ocean	39.7 ± 0.4	254.2	72.7 ± 4	217.2	40.8 ± 0.4	254.2
South Atlantic Ocean	73.2 ± 3.4	152.4	70.1 ± 1.3	279.4	70.2 ± 1.2	279.4
South Pacific Ocean	32.6 ± 0.4	122.4	34.3 ± 1	144.4	32.9 ± 0.4	144.4
Southern Ocean	32.5 ± 1.1	190.4	22.7 ± 0.4	181.8	24.3 ± 0.4	190.4
All oceans	35.6 ± 0.2	254.2	46 ± 0.3	368.2	41.5 ± 0.2	368.2

Table 4
Statistics contrasting active and passive continental margins: escarpments, terraces and continental rise.

| Ocean	Active terrace (km^2)	Passive terrace (km^2)	Active rise (km^2)	Passive rise (km^2)	Active escarpment (km^2)	Passive escarpment (km^2)
Arctic Ocean	0	199,140	0	906,820	0	49,720
Indian Ocean	179,700	557,490	361,100	5,840,740	219,230	422,320
Mediterranean and Black Seas	41,830	8800	174,980	209,930	188,890	29,490
North Atlantic Ocean	49,150	292,000	468,280	7,355,290	500,140	343,340
North Pacific Ocean	250,730	7400	953,620	0	1,470,630	24,460
South Atlantic Ocean	0	275,680	0	6,139,250	38,620	196,920
South Pacific Ocean	84,930	68,410	336,380	0	916,930	83,050
Southern Ocean	4470	33,820	0	6,651,790	94,970	131,970
All oceans	610,800	1,442,740	2,294,360	27,103,820	3,429,390	1,281,260

5.10.2. Stage 2

For each of the possible seamount locations, the base was then calculated based on topographic position index, TPI. TPI was calculated on scales of 5, 10 and 15 cells (ArcGIS → Land Facet Corridor Tools → Topographic Position Index Tools → Calculate TPI Raster, Neighbourhood = Circle, Radius = 5, 10 and 15). Positive TPI scores (above 50–60) were used as the basis for delineation of seamount bases. Based on the above classification of the TPI raster it was converted to a vector layer. The polygons corresponding to potential seamount peaks as identified by the focal statistics and fill methods were selected for further processing. The selected polygons were smoothed (ArcGIS 10 → Cartography Tools → Generalisation → Smooth Polygon, Smoothing Algorithm = PAEK, Smoothing tolerance = 2 nautical miles) and buffered by 1 nautical mile (ArcGIS → Geoprocessing → Buffer,

Linear unit 1 nautical mile). A perimeter/area ratio was calculated to separate seamounts from ridges (as described fully below for "ridges").

The resulting seamount bases were then visually checked against 100 m contours generated from the SRTM30_PLUS model and modified or deleted where the automated methods either failed to properly detect the seamount boundaries or identified non-seamount features.

5.11. Guyots (Supplementary Table 13)

Guyots are "an isolated (or group of) seamount (s) having a comparatively smooth flat top. Also called tablemount(s)" (IHO, 2008). In this study the seamount base layer was used to mask the SRTM30_PLUS model. The gradient of the resulting grid was calculated (ArcGIS 10 → DEM Surface Tools (Jenness et al., 2012) → Slope, Slope
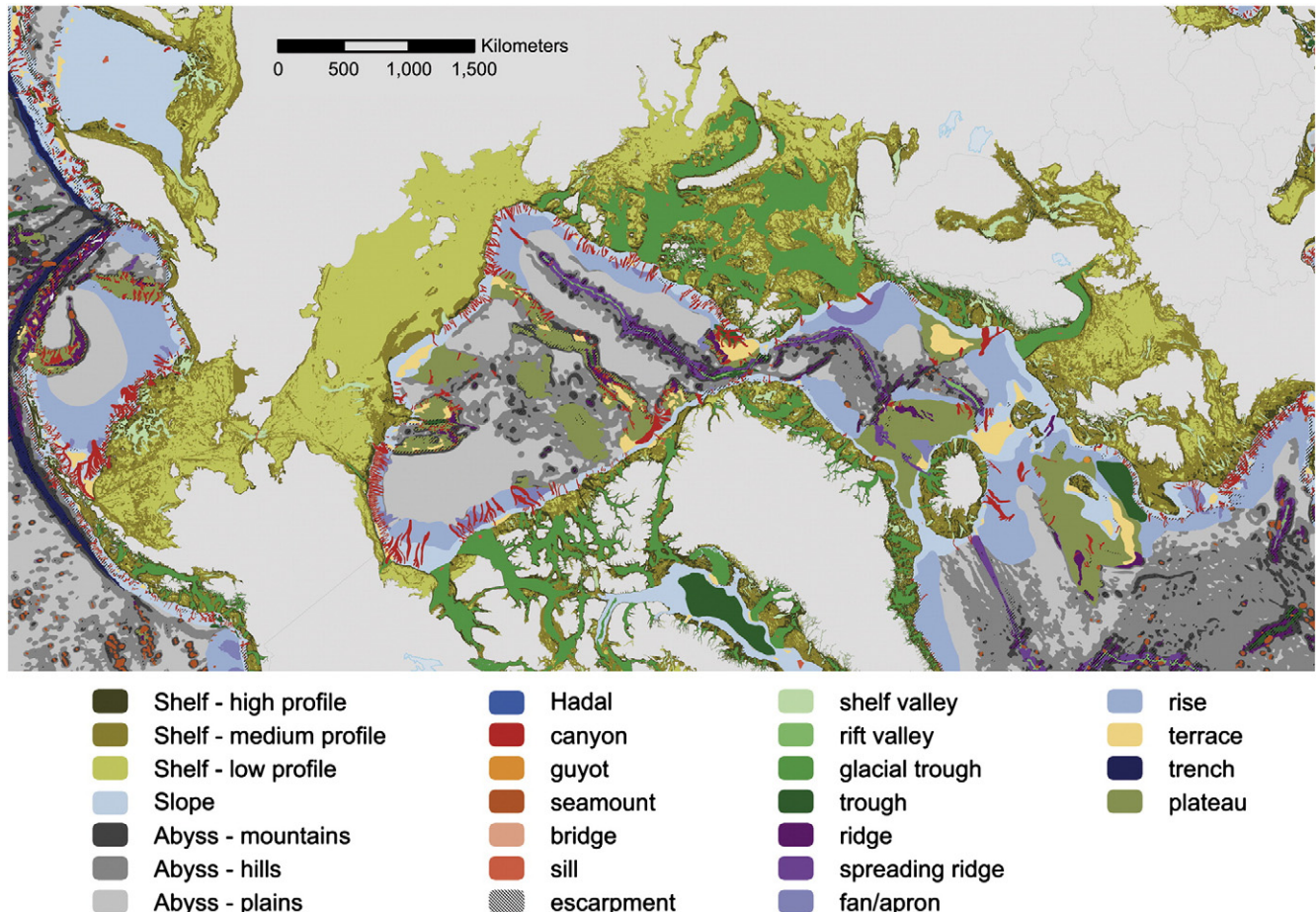
Fig. 5. Geomorphic features map of the Arctic Ocean. Dotted white lines mark boundaries between major ocean regions. Basins are not shown.

computation method = 4-cell method). The gradient was classified into areas of >2° and areas of <2°. The areas less than 2° were converted into vector layers. Where these occurred at the top of seamounts and were greater than a minimum size threshold (10 km²) they were flagged as possible guyots. These possible guyots were then visually checked and either classified as a guyot or a seamount. Additionally the remaining seamounts were visually checked to see whether any with flat tops had been missed in the classification process. The geomorphic features map of Agapova et al. (1979) was used in addition to the GEBCO Gazetteer of geographic names of undersea features (IHO-IOC, 2012), to ensure all previously mapped features were assessed for inclusion in our map.

5.12. Submarine canyons (Supplementary Table 14)

Submarine canyons are defined as "steep-walled, sinuous valleys with V-shaped cross sections, axes sloping outwards as continuously as river-cut land canyons and relief comparable to even the largest of land canyons" (Shepard, 1963). "Large" canyons were mapped in this study based on the definition of Harris and Whiteway (2011), which requires canyons to extend over a depth range of at least 1000 m and to be incised at least 100 m into the slope at some point along their thalweg. Canyon mapping in this study was based on a combination of automated and expert interpretation of the SRTM30_PLUS model. Topographic position index for the SRTM30_PLUS model was calculated for 3, 5 and 10 cell radiuses. For each TPI raster layer, cells with a value of greater than 50 were extracted and converted to vector layers. These three vector layers were then merged to form a single layer that formed the basis for guiding further refinement of the canyons layer. The TPI derived canyon layer was overlayed with 100 m contours generated from the STRM bathymetry. The polygons were then refined to better capture the shape of canyon features, to remove areas that were clearly not canyons and add canyons that were missed. Two categories of submarine canyon were mapped separately: (Feature 22) shelf incising canyons; and (Feature 23) blind canyons.

Shelf incising canyons have heads that cut across the shelf break, and in which there are landward-deflected isobaths on the continental shelf. Blind canyons are those which have heads that are wholly confined to the slope, below the depth of the shelf break. Both categories of canyon may extend across the slope and into abyssal depths and include those parts of canyon–channel systems that are at least 100 m in vertical relief, thus overlapping with fan deposits on the continental rise.

Shelf incising canyons are over twice the mean size of blind canyons on average (780 km² and 380 km², respectively), greater in mean length (54.8 and 37.3 km, respectively) and less deeply incised (1395 and 2963 m, respective mean depths). Canyons in the Mediterranean and Black Seas have the shortest mean length, smallest depth of incision and smallest average area of the ocean regions (for both shelf incising and blind canyons). In contrast, shelf incising canyons in the Arctic Ocean have the greatest mean length, greatest depth of incision and greatest average area. For blind canyons, it is the Southern Ocean that has the greatest mean length, greatest depth of incision and greatest average area.

The ratio of area of shelf-incising to blind canyons indicates that the Mediterranean and Black Seas is the only ocean region where the area of shelf-incising is larger than the area of blind canyons. The South Atlantic has the smallest ratio of 0.289, indicating that shelf-incising canyon area in that region is much less than the area of blind canyons.
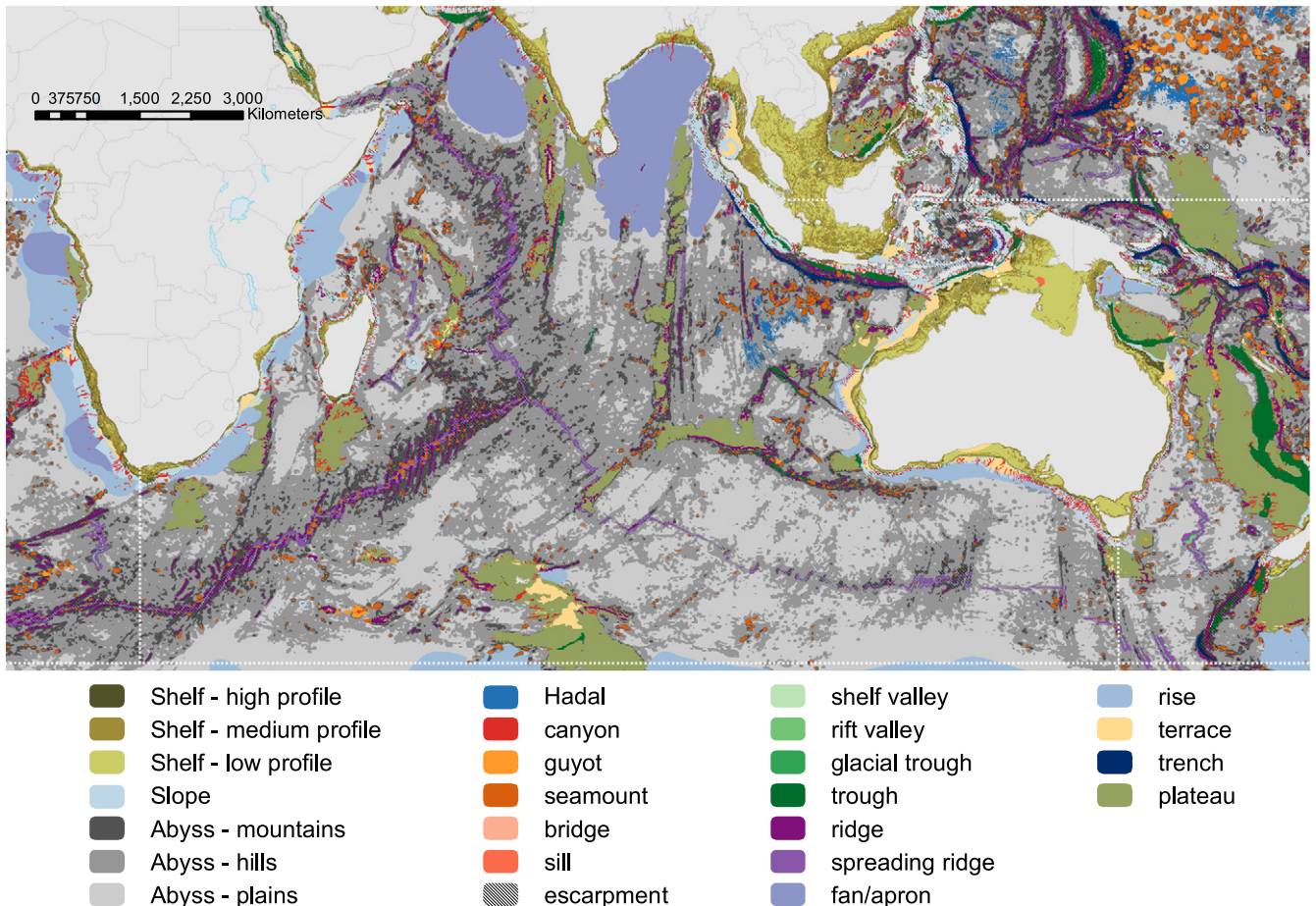

Fig. 6. Geomorphic features map of the Indian Ocean. Dotted white lines mark boundaries between major ocean regions. Basins are not shown.

5.13. Ridges (Supplementary Table 15)

Ridges in this study are confined to "an isolated (or group of) elongated narrow elevation(s) of varying complexity having steep sides, often separating basin features" (IHO, 2008). In this study "ridges" were confined to features greater than 1000 m in relief (i.e. they overlay the abyssal mountains classification layer) and overlap parts of the mid-ocean ridges, which were mapped as a separate feature. Ridges were calculated based on Topographic Position Index (TPI), calculated for 50 and 100 cells (ArcGIS → Land Facet Corridor Tools → Topographic Position Index Tools → Calculate TPI Raster, Neighbourhood = Circle, Radius = 50 and 100). The TPI rasters (TPI50 and TPI100) were reclassified into three classes, greater than −200, −200 to −1000 and less than −1000. The −200 to −1000 and less than −1000 TPI were converted to vector layers. All −200 to −1000 polygons that did not adjoin a less than −1000 polygons were deleted. The remaining polygons were merged. Areas of overlap between the resulting polygons from the TPI50 and TPI100 were then used as the basis for classification of ridges. The polygons were then smoothed (ArcGIS 10 → Cartography Tools → Generalisation → Smooth Polygon, Smoothing Algorithm = PAEK, Smoothing tolerance = 2 nautical miles). The feature polygons were then filtered based on a modified perimeter to area (P/A) ratio to remove those features that were circular or near circular, defined as: $(0.079577472 * P^2) / A$. This resulted in spherical features having a P/A ratio of 1 irrespective of size, and the more elongated or complex a feature is, the greater the value. Features were filtered out if they had a ratio of less than 2.

The remaining features were then filtered on size, with features of <100 km^2 removed. The final ridges were then confirmed as being >1000 m in height at some point along their length and visually checked to ensure there were no artefacts from the data processing.

The GEBCO Gazetteer of geographic names of undersea features (IHO-IOC, 2012) was used to ensure all named features were examined and were manually added by hand where necessary. Features named as "ridges" overlapped with other categories, especially plateaus, seamounts and spreading ridges. Features that were not automatically classified, but which were already captured as belonging to one of these other categories, were not included separately as "ridges". In several cases ridges overlapped with plateaus (i.e. there are ridges superimposed on plateaus). In one case (for the Zapiola Ridge, located in the South Atlantic Ocean), the named feature is less than 400 m in elevation and so this feature was not included as a ridge in our map.

Overall, ridges are most common in the North and South Pacific Oceans, covering 3.50% and 3.00% of the two ocean regions, respectively. The Arctic Ocean and the Mediterranean and Black Sea have the fewest number of ridges and least amount of ridge area (<1%). The largest single ridge feature mapped in this study is an un-named ridge near the Aleutian Islands that covers an area of 63,400 km^2.

5.14. Troughs (Supplementary Table 16)

The IHO (IHO, 2008) definition of a trough is "a long depression of the sea floor characteristically flat bottomed and steep sided and normally shallower than a trench". In this study we found that troughs are also commonly open at one end (i.e. not defined by closed bathymetric contours) and their broad, flat floors may exhibit a continuous gradient along a thalweg. Troughs may originate from glacial erosion processes or have formed through tectonic processes. In this study,
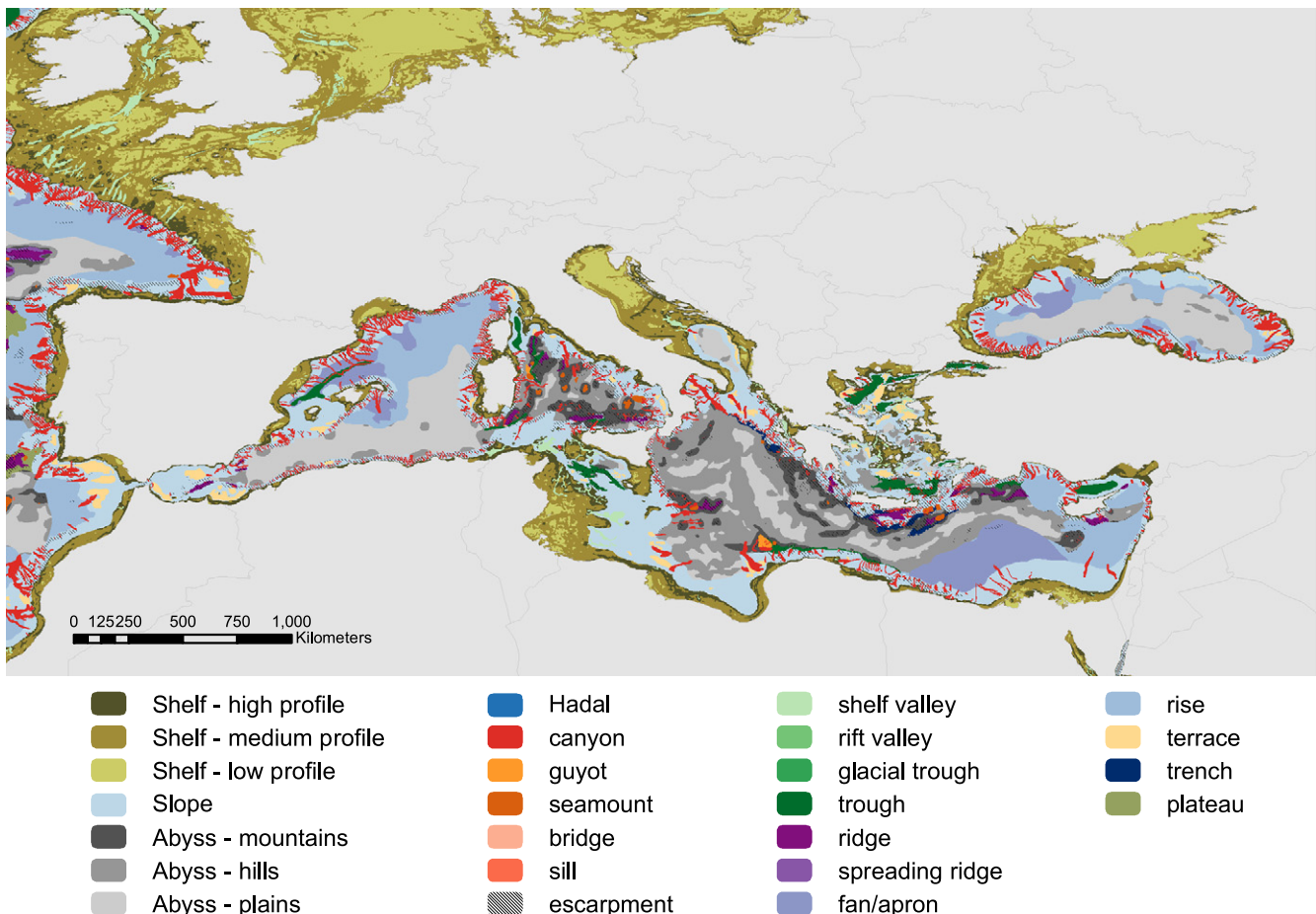

Fig. 7. Geomorphic features map of the Mediterranean and Black Seas. Dotted white lines mark boundaries between major ocean regions. Basins are not shown.

glacial troughs incised into the shelf are a separate category; here we include all troughs not of a glacial origin, typically superimposed on the slope and/or abyssal base layers. Trenches that have been infilled with sediment may evolve into troughs, as appears to have occurred in troughs adjacent to North and South America, for example. Slumping on the sides of some troughs has formed a bridge across the trough, thereby dividing it into two separate sections (see "Bridges" below). In this study all troughs were digitised by hand based on the interpretation of 100 m bathymetric contours.

The 167 troughs mapped in this study cover an area of 2,841,420 km^2. Troughs cover a large fraction of the Mediterranean and Black Seas region whereas the South Atlantic Ocean has the least amount of trough area. Troughs in the South Pacific Ocean have the largest average size, including the New Caledonia and Norfolk Troughs (a single feature) that covers an area of over 500,000 km^2.

5.15. Trenches (Supplementary Table 17)

Trenches are "a long narrow, characteristically very deep and asymmetrical depression of the sea floor, with relatively steep sides" (IHO, 2008). Trenches are generally distinguished from troughs by their "V" shape in cross section (in contrast with flat-bottomed troughs). In this study trenches were mapped by selecting closed bathymetric contours that defined basins contained within the trench feature, and then joining the basin segments together by hand digitising along more elevated sections. In this way, bridge features were also identified (as coinciding with infilled sections of trenches; see section on "Bridges").

A total of 56 trenches were mapped in this study, covering an area of 1,967,350 km^2. Trenches are most common in the North and South

Pacific Oceans, together accounting for 79.8% of all ocean trenches by area. There are no trenches in the Arctic Ocean. The largest trench by map area is the contiguous Kuril–Kamchatka–Aleutian Trench complex, which covers an area of 254,740 km^2.

5.16. Bridges (Supplementary Table 18)

Bridge geomorphic features were first described by Gardner and Armstrong (2011) as blocks of material that partially infill the Mariana Trench in four locations, forming a "bridge" across the trench. In this study we have extended Gardner and Armstrong's (2011) interpretation and applied it to all troughs and trenches and have identified a number of bridge features that appear to partially infill trenches and troughs in the global ocean. Bridges were mapped in conjunction with trenches and troughs as explained above.

5.17. Fans (Supplementary Table 19)

Fans are "a relatively smooth, fan-like, depositional feature normally sloping away from the outer termination of a canyon or canyon system" (IHO, 2008). Since submarine fans are sediment deposits, the NGDC map of global ocean sediment thickness (Divins, 2003) was used to assist with identifying them. Fans overlay and comprise part of the continental rise and are located offshore from the base of the continental slope (Curray et al., 2002; Dowdeswell et al., 2008; Covault, 2011). Fans are inter-related with submarine canyons and sediment drift deposits; in cases where canyon axes extend across the rise, the canyon–channels may be flanked by sediment drift deposits, which have been grouped with fans in this study. Fans are defined in the present study
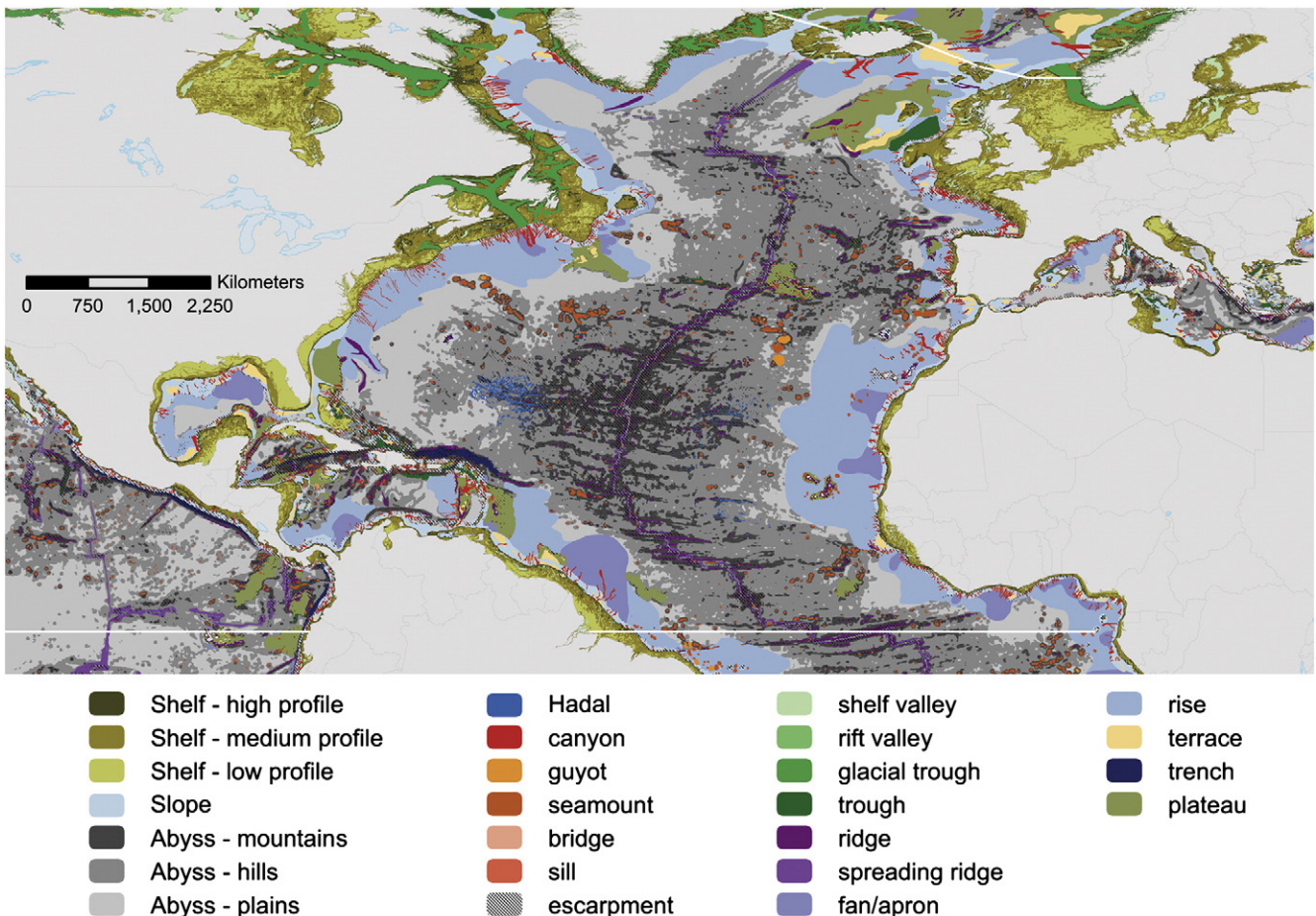

Fig. 8. Geomorphic features map of the North Atlantic Ocean. Dotted white lines mark boundaries between major ocean regions. Basins are not shown.

by 100 m isobaths that form a concentric series exhibiting an expanding spacing in a seaward direction away from the base of the slope, sometimes clearly associated with a canyon mouth, but also comprising low-relief ridges between canyon–channels on the abyssal plain.

5.18. Plateaus (Supplementary Table 20)

Plateaus are "flat or nearly flat elevations of considerable areal extent, dropping off abruptly on one or more sides" (IHO, 2008). Plateaus were digitised by hand based on 100 m contours. In areas where plateaus abut the margin, the foot of slope was allowed to flow offshore to encompass the plateau feature, where a clear seaward dipping gradient was apparent. In other locations marginal plateaus are distinctly separate from the continental slope and form isolated, raised platforms. The geomorphic features map of Agapova et al. (1979) and the GEBCO Gazetteer of geographic names of undersea features were used to ensure all named features were included.

A total of 184 plateaus were mapped in this study, covering an area of 18,486,600 km^2, or 5.11% of the oceans. The largest plateau is located in the South Pacific Ocean, extending from New Zealand to northeast Australia, including Challenger Plateau and Lord Howe Rise (Harris, 2011) and covers a total area of 1,505,370 km^2. Other plateaus of notable size are the Campbell Plateau (1,229,370 km^2) and the Kerguelen Plateau (1,226,230 km^2). Plateaus are generally important features in the South Pacific and Indian Oceans, where they cover areas of over 7% and 8% of those ocean regions, respectively. There were no plateaus mapped in the Mediterranean and Black Seas in this study.

5.19. Coral reefs (Supplementary Table 21)

The coral reefs layer was obtained from the Reefs at Risk Revisited database (WRI, 2011). It was not modified in any way and is included here for convenience for reference purposes. Coral reefs cover an area of 212,340 km^2, or 0.059% of the oceans. Overall, coral reefs are most common in the South Pacific Ocean, covering 0.106% of that ocean region, including 3.63% of the continental shelf. Coral reefs occur in five out of the eight ocean regions but cover significant areas (>10,000 km^2) only in four: the Indian, North Atlantic, North Pacific and South Pacific Oceans.

6. Integrated results

6.1. The new global seafloor geomorphic features map

By integration of the base layers, classification layers and discrete feature layers presented above a new global seafloor geomorphic features map (GSFM) has been created comprised of 131,192 separate polygons (Fig. 4). Although there are numerous possible approaches to assess the GSFM, we focus here on two perspectives of the integrated results to quantify geomorphic differences between passive and active continental margins (Fig. 2), and between the eight different ocean regions selected for detailed analysis.

6.2. Passive and active margins

The geomorphic differences between active and passive continental margins have long been recognized and described by pioneers of marine

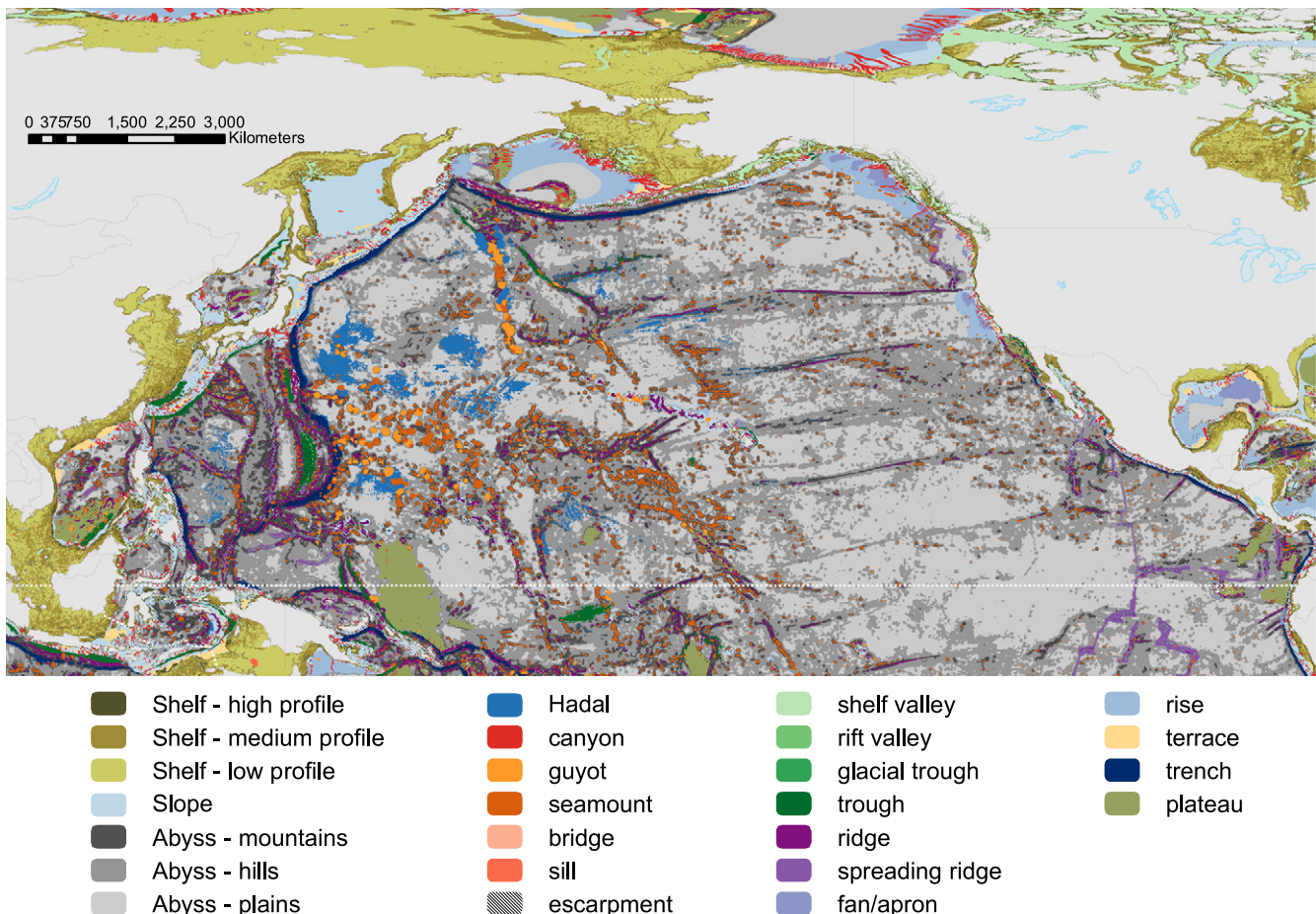|			
Shelf - high profile	Hadal	shelf valley	rise
Shelf - medium profile	canyon	rift valley	terrace
Shelf - low profile	guyot	glacial trough	trench
Slope	seamount	trough	plateau
Abyss - mountains	bridge	ridge	
Abyss - hills	sill	spreading ridge	
Abyss - plains	escarpment	fan/apron	

Fig. 9. Geomorphic features map of the North Pacific Ocean. Dotted white lines mark boundaries between major ocean regions. Basins are not shown.

geology (e.g. Shepard, 1963; Kennett, 1982). Major differences include the width of the shelf (wider on passive margins), the steepness of the slope (steeper on active margins), the occurrence of continental rise (most common on passive margins) and the presence of ocean trenches (associated with active margins and absent from passive margins). A recent global study of submarine canyons (Harris and Whiteway, 2011) found that active continental margins contain over 50% more canyons (by number) than passive margins and the canyons are steeper, shorter, more dendritic and are more closely spaced on active than on passive continental margins.

The GSFM supports all of these previous observations with additional quantitative estimations of feature area and other relevant dimensions. Shelf width in this study was measured using an ArcGIS algorithm that measured the distance to the nearest land from the shelf break. The width of the continental shelf is nearly three times wider on passive margins (88 km) than active margins (31 km; Table 2). The ocean region having the widest (passive margin) shelves is the South Atlantic (123 km) and the most narrow (active margin) shelves are in the Mediterranean and Black Seas (11 km; Table 2). The widest shelf is in the Weddell Sea in Antarctica at 778 km.

The width of the continental slope was estimated using ArcGIS by finding the shortest distance at regular intervals between the shelf break and foot of slope. On average, the slope is a narrow band 41 km wide that encircles all continents and islands (Table 3). The passive margin slopes of the South Atlantic Ocean are the widest on average (73 km) although the slope attains its greatest width of 368 km in the North Atlantic, where the slope protrudes south of Newfoundland. The most narrow active margin slopes are in the Mediterranean and Black

Seas (25.8 km; Table 3). The average width of active slopes (35.6 km) is somewhat less the average width of passive margin slopes (45.7 km).

The steepness of the slope is estimated here based on the area of escarpment (slope having a gradient >5°). Our results indicate that active margin slopes contain over 3.4 million km^2 of escarpment, compared with less than 1.3 million km^2 of escarpment on passive slopes (Table 4). The continental rise covers more than 27.1 million km^2 adjacent to passive margins and less than 2.3 million km^2 adjacent to active margins. Terraces are also more common on passive margins than on active margins (Table 3). These absolute area estimates must be viewed in the context that the approximate proportions of active and passive margins are not equal; we estimate that the Earth's margins are approximately 35% active and 65% passive (Fig. 2).

6.3. Geomorphic characteristics of ocean regions

Spatial analysis of the GSFM indicates variation in the relative proportions of geomorphic features between ocean regions, whereby each region is characterised by features that are dominant, rare or absent (Figs. 5–12). In terms of absolute area (Table 5), the South Pacific (Fig. 11), being the largest ocean, tends to also have the greatest absolute value of feature area. In fact, the largest absolute area of 11 feature categories occurs in the South Pacific; the North Pacific (Fig. 9) has the largest absolute area of 9 feature categories. Next comes the North Atlantic (Fig. 8), which has the largest area of shelf, rise, medium-profile shelf and shelf valleys (Table 5). The Indian Ocean (Fig. 6) has the largest area of submarine fan, including the world's two largest submarine fans, the Bengal and Indus (Curray et al., 2002; Covault, 2011). It also has the
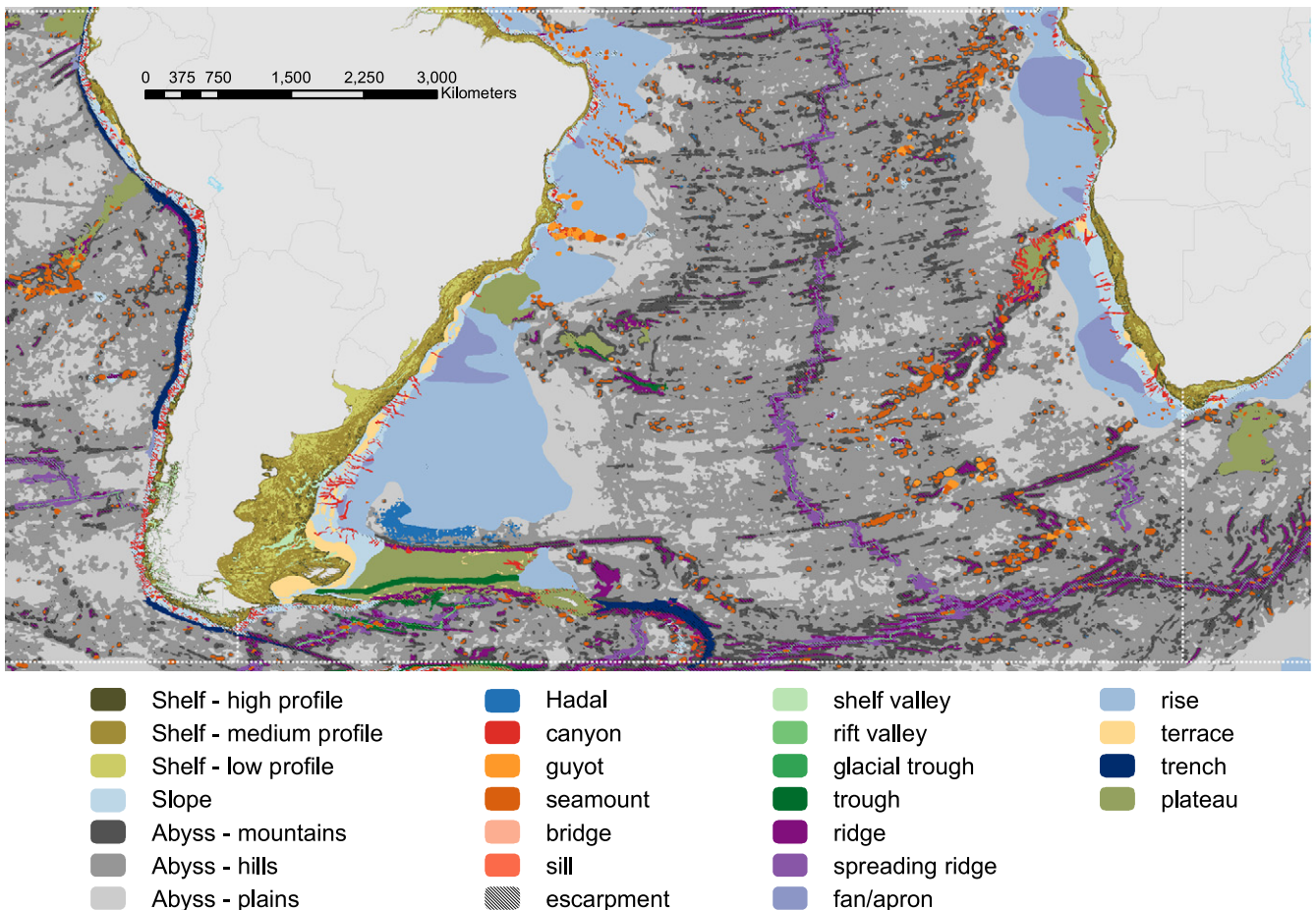

Fig. 10. Geomorphic features map of the South Atlantic Ocean. Dotted white lines mark boundaries between major ocean regions. Basins are not shown.
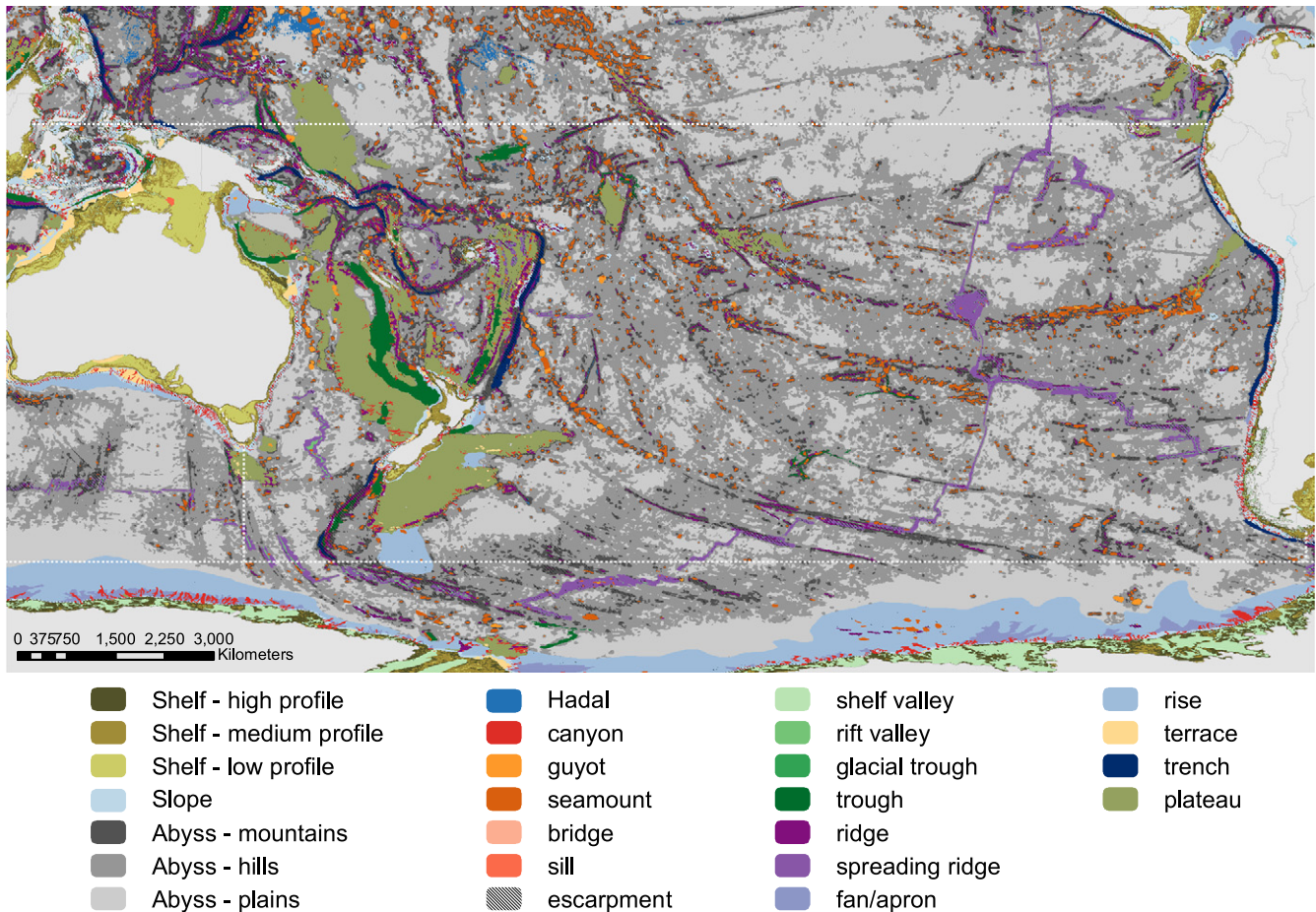
Fig. 11. Geomorphic features map of the South Pacific Ocean. Dotted white lines mark boundaries between major ocean regions. Basins are not shown.

largest area of slope terraces and rift valleys. Finally, the Arctic Ocean has the largest absolute area of glacial troughs (Table 6) and the Southern Ocean (Antarctica; Fig. 12) has the greatest area of high-profile shelf (Table 5).

In terms of the smallest absolute areas of features, the Mediterranean and Black Seas (Fig. 7), being the smallest of the 8 ocean regions, also have the greatest number in this category. In fact, 20 out of 30 of the smallest absolute areas of features occur in the Mediterranean and Black Seas (Table 5). The second smallest ocean region, the Arctic Ocean (Fig. 5), has 6 of the smallest absolute areas of features. The Southern Ocean (Fig. 12) has the smallest absolute area of continental slope, terraces and low-profile shelf. The South Atlantic has the smallest area of shelf-incising canyons and the South Pacific has the smallest area of submarine fans (Table 5).

Normalising the feature areas as a percentage of ocean region area produces a different perspective of ocean region characteristics (Table 6). The North Pacific (Fig. 9) and Arctic Oceans (Fig. 5) each have 7 of the greatest percentage areas of the 29 geomorphic feature types (Table 6). The Arctic Ocean also has 10 of the least percentage areas of the 29 geomorphic feature types. This makes the Arctic Ocean the most "unusual" of the eight ocean regions from a geomorphological perspective. In contrast, the North Atlantic (Fig. 8) is the most "average", as it does not contain the greatest or smallest percentage area of any of the 29 geomorphic feature types mapped in our study (Table 6). The South Pacific (Fig. 11), the largest ocean region, has only three of the greatest feature areas as a percentage of ocean region (abyss, abyssal hills and coral reefs) whereas the Mediterranean and Black Seas, the smallest ocean region, has four of the greatest feature areas (slope, basin, escarpment and trough; Table 6).

6.4. Seafloor roughness

Two separate indicators of seabed roughness are used in this study: seabed relief and gradient. The continental shelf is divided into three roughness categories based on vertical relief: low profile < 10 m; medium profile 10–50 m; and high profile > 50 m. The three subdivisions of the abyssal zone are also based on vertical relief: abyssal plains (0–300 m relief); abyssal hills (300–1000 m); and abyssal mountains (>1000 m). The Antarctic shelf has the greatest percentage area of high (>50 m) relief (69.3%), which is consistent with that shelf being more than 40% glacial troughs (Table 6). In contrast, although the Arctic shelf also contains large areas of glacial troughs (24.3% of the shelf area; Table 5) it has the greatest percentage area of low (<10 m) relief (45.0%), which occurs mainly in the East Siberian Sea (Fig. 5) where continental ice sheets were not significant agents of shelf erosion during the late Pleistocene (Gualtieri et al., 2003; Niessen et al., 2013).

A seafloor gradient exceeding 5° over an area of >100 km^2 in slope, abyssal and hadal zones is classified here as an "escarpment". Across all oceans the continental slope contains 3268 escarpments characterising 25.1% of slope area (Table 7). Escarpments cover 42.8% of continental slope area in the South Pacific Ocean compared with only 3.62% in the Arctic Ocean (Table 7); thus the Arctic Ocean has the world's most gentle gradient slope. Plotting the percentage area of escarpment versus the area of abyssal hills and mountains provides a broad measure of abyssal ocean floor roughness (Fig. 13), showing that the Arctic and Southern Oceans are the least rough whereas the North Pacific and the Mediterranean and Black Sea regions are most rough.
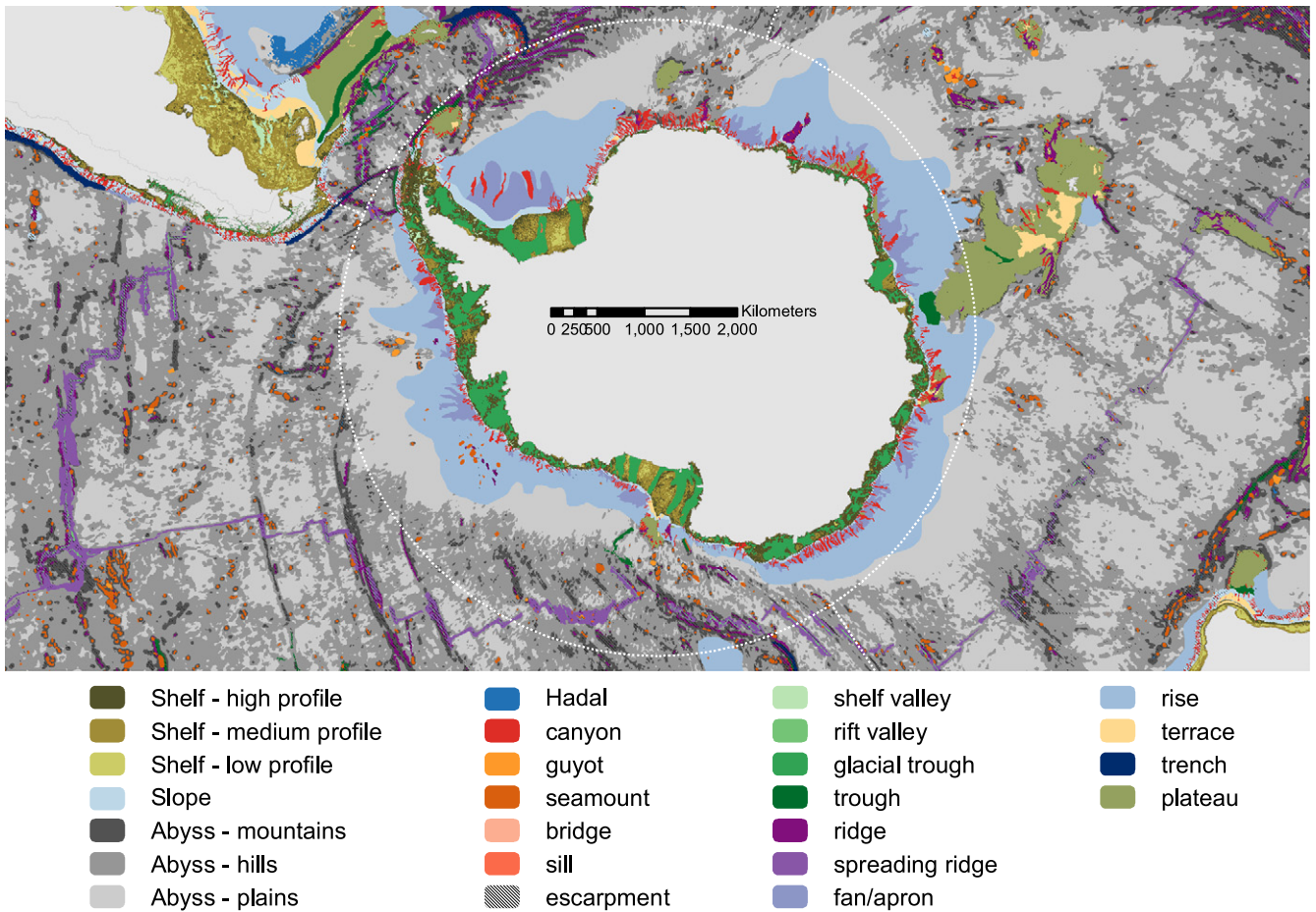
Fig. 12. Geomorphic features map of the Southern Ocean. Dotted white lines mark boundaries between major ocean regions. Basins are not shown.

7. Discussion

Of the many purposes for mapping seafloor geomorphic features, four stand out: (1) to support government spatial marine planning, management and decision-making; (2) to support and underpin the design of Marine Protected Areas (MPA); (3) to generate knowledge about benthic ecosystems and seafloor geology; and (4) to conduct assessments of living and nonliving seabed resources including economic valuation (Harris and Baker, 2012). The new GSFM applies to all four of these purposes. However, the focus of this discussion is to illustrate how the GSFM can be used to generate new knowledge about seafloor geomorphology by showing an example of three different approaches: first, observations of rift valley segmentation are combined with an available dataset on seafloor spreading to explore formative processes; second, a spatial analysis of polar and non-polar continental margins demonstrates significant geomorphic differences; and third, comparisons will be made of seamount and guyot statistics from the present study with the results of previous studies.

7.1. Mid-ocean ridge rift valley segmentation and seafloor spreading

The mid-ocean ridge covers an area of 6,699,460 km^2, equal to 1.85% of the seafloor (Table 5). We mapped 658 separate rift valley segments, found mainly along mid-ocean ridges, covering an area of 710,060 km^2. Segmentation of the rift valley, due to transform faults and other factors (Macdonald, 2001), is manifest as a greater number of smaller-sized segments in the Indian, North Pacific and South Pacific Oceans, compared with the Arctic, North Atlantic and South Atlantic Oceans, where rift valleys are fewer in number (less segmented) and much greater in size than the global average (Table 8). Earth's largest mid-ocean rift valleys

occur in the Atlantic Ocean and they are up to 21,390 km^2 in area, compared with the global mean size of only 1080 km^2 (Table 8), although, as noted above, the Indian Ocean contains the largest absolute area of rift valleys.

We used the EarthByte (Müller et al., 1997) database on mid-ocean ridge spreading rates to assign a mean spreading rate to each of the 658 rift valley segments and to then estimate a mean rift valley segment size and spreading rate for each major ocean region. The results (Fig. 14A) demonstrate that larger rift valley segments are generally associated with slow-spreading rates and smaller rift valley segments are associated with fast spreading. The relationship appears to generally hold true but is complicated by other factors that include crustal thickness, the development of fracture zones and patterns of upwelling magma (Macdonald, 2001). Our data indicate that Order 3 rift valley segments (as per Macdonald, 2001) are the most abundant (Fig. 14B), although the 1 km bathymetric grid size used is too coarse to resolve Order 4 rift valley segments.

7.2. Continental glaciation and polar submarine geomorphology

Continental glaciations have had a clear influence on submarine geomorphology at slope to abyssal depths, based on our analysis. This influence extends well beyond the occurrence of glacial troughs incised into polar continental shelves (Figs. 5 and 12), and is apparent throughout slope and abyssal depths, as reflected in abyssal roughness (Fig. 13), the physiography of submarine canyons, the occurrence of fans and extensive continental rise and abyssal plains at abyssal depths adjacent to polar margins.

Polar submarine canyons are twice the size of those in non-polar regions. Canyons in the Arctic have an average size of 890 km^2 and in the

Table 5
List of global areas of seafloor geomorphic features, definitions from the IHO (2008) and other references cited, total area and the percentages of total ocean area represented by each feature category. The sum of the area of mutually exclusive base layers (shelf, slope, abyss and hadal zones, yellow shading) equals 361,883,510 km², which is the total mapped ocean area. All other feature layers are superimposed on the four base layers and are listed in order of decreasing area. Regions where features attain their greatest total area are shaded red and regions where features attain their smallest total area (or are absent) are shaded blue.

Feature category	Definition	Global Area Area	% Area	Arctic km²	Indian km²	Mediterranean km²	North Atlantic km²	North Pacific km²	South Atlantic km²	South Pacific km²	Southern Ocean km²
Ocean area	Total mapped area.	361,883,510	100	12,990,480	71,297,430	3,022,510	44,766,460	81,913,850	40,413,850	87,142,840	20,335,240
Shelf	A zone adjacent to a continent (or around an island) and extending from the low water line to a depth at which there is usually a marked increase of slope towards oceanic depths.	32,242,540	8.91	6,727,440	4,047,570	709,990	7,313,790	6,144,810	2,036,140	2,547,450	2,715,360
Slope	The deepening sea floor out from the shelf edge to the upper limit of the continental rise, or the point where there is a general decrease in steepness.	19,606,260	5.42	913,590	4,189,700	906,590	3,436,150	4,752,240	1,591,830	3,201,000	615,170
Abyss	Area of seafloor located at depths below the foot of the continental slope and above the depth of the hadal zone.	306,595,900	84.7	5,349,450	62,811,460	1,405,930	33,720,840	68,720,670	36,576,710	81,007,450	17,003,390
Hadal	Seafloor occurring at depths >6000 m.	3,437,930	0.95	0	248,700	0	295,680	2,296,130	209,170	386,940	1320
Basin	A depression, in the sea floor, more or less equidimensional in plan and of variable extent defined by a closed bathymetric contour.	158,529,660	43.8	3,809,710	33,051,130	1,648,220	17,955,140	34,175,490	18,056,480	39,533,570	10,299,940
Abyssal hills	Variation in relief over a 25-cell radius of 300–1,000 m.	149,451,310	41.3	2,244,920	30,179,170	613,830	16,477,470	29,676,230	19,511,510	44,059,800	6,688,370
Abyssal plains	Variation in relief over a 25-cell radius of <300 m.	100,863,730	27.9	2,068,570	21,772,790	612,870	10,255,540	24,906,630	10,033,650	22,648,400	8,565,270
Abyssal mountains	Variation in relief over a 25-cell radius of >1,000 m.	57,678,740	15.9	1,036,060	10,859,500	179,220	6,987,830	14,137,990	7,031,560	14,299,470	1,749,840
Rise	Low gradient, evenly-spaced, slope-parallel contours extending seawards from the foot of the continental slope generally confined to areas of sediment thickness >300 m based on the sediment thickness map of Divins (2003).	29,832,040	8.24	906,830	6,244,200	384,910	7,823,570	976,910	6,234,080	556,710	6,704,840
Escarpment	An elongated, characteristically linear, steep slope >5 and areal extent of >100 km², separating horizontal or gently sloping sectors of the sea floor in non-shelf areas.	21,151,400	5.84	204,820	3,271,020	245,040	2,739,990	6,461,170	1,935,470	5,594,040	699,850
Plateau	Flat or nearly flat elevations of considerable areal extent, dropping off abruptly on one or more sides.	18,486,610	5.11	1,193,740	5,036,870	0	1,628,360	1,856,790	1,220,230	7,054,800	495,830
Shelf - medium profile	Variation in relief over a five-cell radius of 10–50 m.	14,447,690	3.99	2,592,830	2,065,880	321,860	3,771,720	2,815,700	1,298,480	836,160	745,060
Shelf - low profile	Variation in relief over a five-cell radius of <10 m.	9,799,870	2.71	3,033,170	1,154,310	136,550	1,839,010	2,141,570	436,310	969,350	89,610
Ridge	An isolated (or group of) elongated (length/width ratio >2), narrow elevation(s) of varying complexity having steep sides, >1,000 m in vertical relief.	9,770,720	2.70	118,050	1,747,480	26,460	990,440	2,873,990	1,081,370	2,616,730	316,200
Fan	A relatively smooth, fan-like, depositional feature commonly found sloping away from the outer termination of a canyon or canyon system.	8,303,160	2.29	152,270	4,342,910	165,830	1,325,520	236,530	895,640	25,560	1,158,890
Shelf - high profile	Variation in relief over a five-cell radius of >50 m.	7,995,050	2.21	1,101,450	827,450	251,580	1,703,060	1,187,560	301,350	741,860	1,880,730
Seamount	A discrete (or group of) large isolated elevation(s), greater than 1000 m in relief above the sea floor, characteristically of conical form (length/width ratio <2).	7,859,200	2.17	5380	966,990	7700	509,200	3,097,050	790,690	2,330,400	151,780
Spreading ridge	The linked, major mid-oceanic mountain systems of global extent coinciding with the youngest ocean crustals mapped by Mülleret al. (1997).	6,699,460	1.85	254,630	1,547,910	0	677,630	840,300	1,166,750	1,868,490	343,740
Shelf valley	Valleys incised more than 10 m into the continental shelf.	4,756,290	1.31	189,920	120,430	25,490	354,200	249,460	83,920	60,980	43,150
Canyon	Steep-walled, sinuous valleys with V-shaped cross sections, axes sloping outward as continuously as river-cut land canyons and relief comparable to even the largest of land canyons (Shepard, 1963). (A) total canyon area; (B) blind, slope-confined. (A)	4,393,650	1.21	359,650	760,420	163,040	738,430	816,580	291,290	694,790	569,440
	(B)	1,613,860	0.45	162,020	222,690	94,430	292,330	367,710	65,320	214,960	194,410
	(C)	2,779,790	0.77	197,630	537,740	68,610	446,100	449,220	225,830	479,640	375,020
Glacial trough	Elongate troughs, typically trending across the continental shelf, attributed to glacial erosion during the Pleistocene ice ages (Hambrey, 1994).	3,659,360	1.01	1,634,770	0	0	740,090	134,710	20	27,360	1,091,790
Trough	A long depression of the seafloor characteristically flat bottomed and steep sided, generally open at one end.	2,841,420	0.785	62,790	412,660	63,830	366,790	572,970	149,200	1,116,670	96,520
Terrace	An isolated (or group of) relatively flat horizontal or gently inclined surface(s), sometimes long and narrow, which is (are) bounded by a steeper ascending slope on one side and by a steeper descending slope on the opposite side.	2,303,490	0.637	224,980	896,730	50,630	343,410	274,570	286,400	188,480	38,290
Trench	A long narrow, characteristically very deep and asymmetrical depression of the sea floor, with relatively steep sides.	1,967,350	0.544	0	166,580	14,970	116,350	824,720	91,240	745,810	7690
Guyot	A seamount having a flat top >10 km² in areal extent and with a gradient of <2°.	936,920	0.259	0	67,010	2800	31640	499,990	133,710	187,900	13,870
Rift valley	Valleys confined to the central axis of mid-ocean spreading ridges; they are elongate, local depressions flanked generally on both sides by ridges.	710,060	0.196	33,270	165,220	0	108,110	102,140	118,690	156,220	26,420
Sill	A sea floor barrier of relatively shallow depth restricting water movement between basins.	45,450	0.0126	6630	1280	120	8180	6650	3000	14,430	5160
Bridge	Features composed of blocks of material that partially infill trenches or troughs, forming a "bridge" across them (Gardner and Armstrong, 2011).	8,270	0.00229	50	2240	270	210	2410	60	2850	170
Coral reef	Coral reefs from WRI (2011).	212,340	0.0587	0	49,970	0	22,380	46,930	1090	91,980	0

Southern Ocean the average canyon size is 997 km², compared to the overall (global) average size of 463 km² (Table 9). The largest submarine canyon on Earth is the Bering–Bristol–Pribylov Canyon complex (Normark and Carlson, 2003), which we estimate has an area of 33,340 km². In fact Earth's largest four canyons are all located on polar slopes that have been influenced by sediment derived from glaciated catchments during the Quaternary.

We mapped 9477 canyons in this study and have generated new data on canyon area, thalweg length and depth of incision, for two separate categories: 2076 shelf-incising canyons and 7401 blind canyons (that incise the slope only). Canyons comprise an average of 11.2% of the continental slope area, attaining maxima of 16.1% of the continental slope of the Arctic Ocean and 15.1% of the Southern Ocean (Antarctic) continental slope. In contrast, the slope of the South Atlantic Ocean has only 8.9% of its area incised by canyons (Table 9).

Polar, shelf-incising canyons are more deeply incised into the slope, to mean depths of around 1600 m and are greater in average length than non-polar canyons (Table 9). Polar canyons, however, have the

Table 6
Summary of features by percentage of surface area in ocean regions and as a global average. The highest and lowest values in each row (for each feature) are indicated by red and blue shading, respectively.

	Arctic Ocean	Indian Ocean	Mediterranean and Black Sea	North Atlantic Ocean	North Pacific Ocean	South Atlantic Ocean	South Pacific Ocean	Southern Ocean	Global average
Shelf	51.8	5.68	23.5	16.3	7.50	5.04	2.92	13.4	8.91
Slope	7.03	5.88	30.0	7.68	5.80	3.94	3.67	3.03	5.42
Abyss	41.2	88.1	46.5	75.3	83.9	90.5	93.0	83.6	84.7
Hadal	0	0.353	0	0.660	2.81	0.508	0.443	0.00650	0.950
Basin	29.3	46.4	54.5	40.1	41.7	44.6	45.4	50.7	43.8
Abyssal hills[1]	42.0	48.3	43.7	49.3	44.2	53.5	54.5	39.3	49.1
Abyssal plains[1]	38.7	34.7	43.6	30.3	37.3	27.7	28.0	50.4	33.2
Abyssal mountains[1]	19.3	17.0	12.7	20.4	18.5	18.8	17.5	10.3	17.7
Rise	17.0	9.94	27.4	23.3	1.42	17.0	0.687	39.4	9.73
Escarpment	1.48	4.59	8.11	6.12	7.88	4.79	6.42	3.44	5.84
Plateau	9.19	7.06	0	3.64	2.26	3.02	8.09	2.44	5.11
Shelf – medium relief[2]	38.5	51.0	45.3	51.6	45.8	63.7	32.7	27.4	44.8
Shelf – low relief[2]	45.0	28.5	19.2	25.1	34.9	21.3	38.2	3.30	30.4
Ridge	0.909	2.45	0.875	2.21	3.50	2.67	3.00	1.55	2.70
Fan	1.17	6.09	5.49	2.96	0.288	2.21	0.0293	5.70	2.29
Seamount	0.0415	1.36	0.255	1.18	3.97	2.00	2.70	0.791	2.23
Shelf – high relief[2]	16.4	20.4	35.4	23.3	19.3	15.0	29.0	69.3	24.8
Spreading Ridge	4.76	2.46	0	2.01	1.22	3.19	2.31	2.02	2.19
Shelf Valley[2]	14.0	0.169	0.843	2.44	0.468	0.208	0.101	5.58	1.31
Canyon[3]	16.1	11.2	13.8	10.4	11.2	8.9	10.2	15.1	11.2
Guyot	0	0.0940	0.0927	0.0269	0.417	0.282	0.189	0.0234	0.195
Glacial Trough[2]	24.3	0	0	10.1	2.19	0.000800	1.08	40.2	11.3
Trough	0.483	0.579	2.11	0.819	0.699	0.369	1.28	0.475	0.785
Terrace[2]	24.6	21.4	5.58	9.75	5.66	18.0	5.81	6.22	11.6
Trench	0	0.234	0.495	0.260	1.01	0.226	0.856	0.0378	0.543
Rift Valley	0.256	0.232	0.00	0.241	0.125	0.293	0.179	0.130	0.196
Coral Reef[2]	0	1.23	0	0.306	0.764	0.0530	3.63	0	0.659
Sills[4]	64	18	13	88	73	8	32	95	391[5]
Bridges[4]	2	12	18	16	33	4	32	8	125[5]

[1] Three abyssal roughness categories are reported as percentage of abyssal area within ocean regions.
[2] Three shelf roughness categories and shelf-confined features reported as percentage of shelf area within ocean regions.
[3] Slope-confined/slope characteristic features reported as percentage of slope area within ocean regions.
[4] Bridges and sills are reported by number of occurrences.
[5] Total number of features.

Fig. 13. Seafloor roughness measured in this study as a function of escarpment percent area of ocean regions, and the sum of percentage area of the abyssal zone that is classified as abyssal hills and abyssal mountains (see Table 5 for data).

Southern Ocean (Table 6), forming a halo of sediment surrounding the continent (Fig. 12). Together, the occurrence in Polar Regions of twice the average size of submarine canyons in association with low roughness (Fig. 13) and with spatially extensive fan, rise and abyssal plain sediment deposits, implies the importance of (glacial) sediment export to the deep sea as a controlling factor in slope and abyssal geomorphology during the Cenozoic.

An interesting observation is that whilst polar submarine canyons are the largest on Earth, the pattern for shelf incising and blind canyons is reversed between the Arctic and Antarctic: whereas shelf incising canyons in the Arctic Ocean have the greatest mean length, greatest depth of incision and greatest average area, for blind canyons it is the Antarctic that has the greatest mean length, greatest depth of incision and greatest average area (Table 9). If shelf incising canyon formation is controlled by the rate of sediment discharge onto the slope (Harris and Whiteway, 2011), it is perhaps the difference in timing of sediment input between the Arctic and Antarctic that explains the observed geomorphic difference. Whereas continental glaciation and consequent sediment input to the Arctic margin has occurred mainly during the Pleistocene, the Antarctic glaciation has been ongoing for the last 40 million years but sediment discharge to the slope probably reached a peak in the middle Miocene to early Pliocene and has dramatically decreased in the late Pleistocene (Cooper and O'Brien, 2004). Whether or not the large, blind canyons of the Antarctic margin are the evolutionary products of shelf incising canyons that have been disconnected from terrigenous (glacial) sediment input over geologic timescales is a question for future researchers.
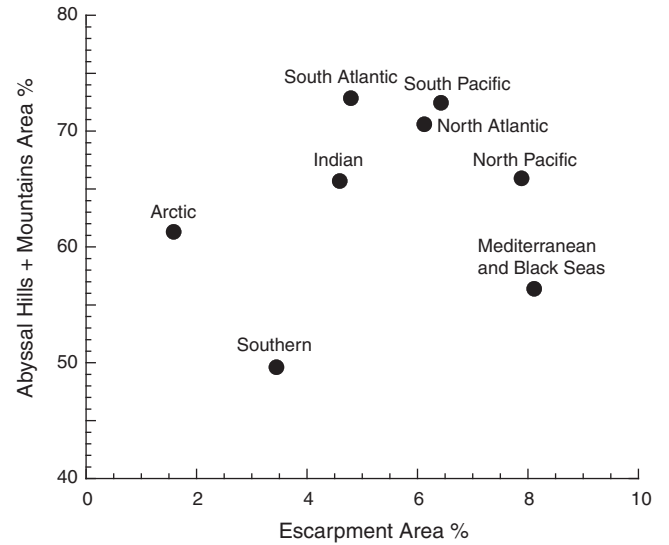
least percentage of escarpment area (Table 7). Escarpments characterise 18.7% of submarine canyons globally and cover 29.1% of canyons in the Mediterranean and Black Seas (Table 7). By comparison, the Arctic Ocean has the smallest proportion of its submarine canyon area as escarpments, equal to just 4.41% and the Southern Ocean (Antarctic) canyons contain only 7.59% escarpment (Table 7).

Features associated with submarine canyons include submarine fans of which 151 were mapped in this study, covering an area of 8,303,160 km^2, or 2.29% of the seafloor. Fans associated with glacial troughs (trough–mouth fans) in the Arctic and Antarctic regions (Hambrey, 1994; Anderson, 1999; Dowdeswell et al., 2008; Figs. 5 and 12) are parts of the continental rise, which covers an area of 29,832,040 km^2, equal to 8.24% of the seafloor (Table 5). The continental rise completely surrounds Antarctica covering 39.4% of the

Table 7
Selected statistics on escarpments. The percentage areas refer to the percentage of ocean region or geomorphic feature that is escarpment.

Ocean	Escarpments on slope (km^2)	Slope that is escarpment (%)	No. of slope escarpments	Escarpments in canyons (km^2)	Canyon that is escarpment (%)
Arctic Ocean	33,100	3.62	58	15,860	4.41
Indian Ocean	775,980	18.5	637	133,380	17.5
Mediterranean and Black Seas	180,620	19.9	170	47,400	29.1
North Atlantic	630,680	18.4	402	146,380	19.8
North Pacific	1,519,700	31.3	871	228,180	27.9
South Atlantic	264,750	16.6	175	32,280	11.1
South Pacific	1,387,760	42.8	817	174,280	25.1
Southern Ocean	177,400	28.8	138	43,200	7.59
All oceans	4,970,000	25.3	3268	820,960	18.7

Table 8
Rift valley statistics. Spreading rate (±standard deviation) is from the EarthByte database (Müller et al., 1997), with average values calculated for each spreading ridge segment.

Ocean	Area (km^2)	Rift valley area (%)	Number of rift valley segments	Average area of rift valley segments (km^2)	Spreading rate (mm/yr)
Arctic Ocean	33,270	0.256	22	1510	7.4 ± 3.8
Indian Ocean	165,220	0.232	155	1070	25.0 ± 17.6
North Atlantic	108,110	0.241	37	2920	15.5 ± 8.8
North Pacific	102,140	0.125	118	870	43.2 ± 29.4
South Atlantic	118,690	0.293	71	1670	22.0 ± 12.7
South Pacific	156,220	0.179	228	690	62.9 ± 31.0
Southern Ocean	26,420	0.130	34	780	30.6 ± 15.8
All oceans	710,060	0.196	658	1080	

7.3. Seamounts, guyots, and ridges

Features characterising the abyssal zone of particular interest for resources and conservation value are seamounts and guyots (Hein et al., 2010; Clark et al., 2011; Yesson et al., 2011). A total of 10,234 seamounts and guyots were mapped in this study, covering a total area of 8,796,150 km^2. Overall, seamount and guyot coverage is greatest as a proportion of seafloor area in the North Pacific Ocean, equal to 4.39% of that ocean region (Table 10; Fig. 9). The Arctic Ocean has only 16

Fig. 14. A). Mean rift valley area versus EarthByte modelled seafloor spreading rate (Müller et al., 1997); ellipses of mean and standard deviation for major ocean regions illustrate that Atlantic rift valley segments are larger and slower-spreading than Pacific segments. B). Histogram of rift valley segments classified by length, mapped in the present study, with Order length categories after Macdonald (2001). Order 4 rift valley segments (scaled to <10 km length) are poorly resolved in the present study.

seamounts and no guyots, and the Mediterranean and Black Seas together have only 23 seamounts and 2 guyots. The 9951 seamounts mapped cover an area of 8,088,550 km^2. Seamounts have on average an area of 790 km^2, with the smallest seamounts found in the Arctic Ocean and the Mediterranean and Black Seas, whilst the largest mean seamount size occurs in the Indian Ocean (890 km^2). The largest seamount has an area of 15,500 km^2 and it occurs in the North Pacific.

There are 283 guyots covering a total area of 707,600 km^2. Guyots have an average area of 2500 km^2, more than twice the average area of seamounts. Nearly 50% of guyot area and 42% of the number of guyots occur in the North Pacific Ocean, covering 342,070 km^2 (Table 10). The largest three guyots are all in the North Pacific: the Kuko Guyot (estimated 24,600 km^2), Suiko Guyot (estimated 20,220 km^2) and the Pallada Guyot (estimated 13,680 km^2).
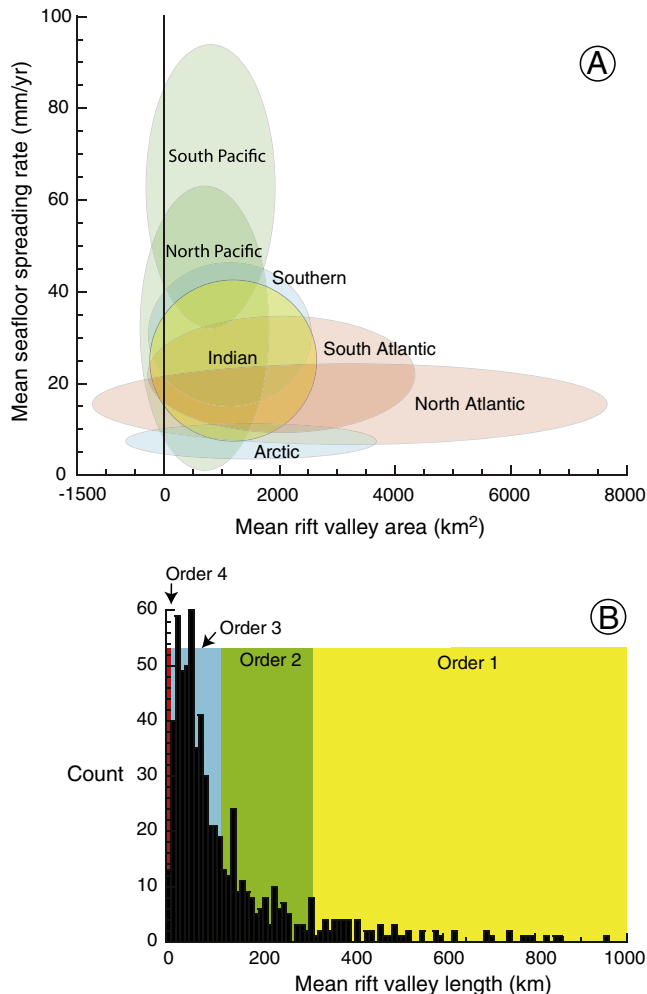
Our seamount number is close to the estimates of Wessel (2001); n = 11,880, but is somewhat less that the number estimated by Kitchingman and Lai (2004); n = 14,287 and much less than that of Yesson et al. (2011) who estimated the global number of seamounts to be 33,452. The total area of seamounts, furthermore, is estimated by Yesson et al. (2011) to be about 17.2 million km^2. Etnoyer et al. (2010) used a simple geometric approach to estimate the area of Wessel (2001) 11,880 seamounts to be about 10 million km^2, a figure which is similar to the area estimated in this study. How can we explain these differences?

The reason is because we have distinguished between seamounts and ridges (see Methods) whereas Yesson et al. (2011) did not treat ridges and seamounts as separate feature categories. We strictly applied the IHO (2008) definition of seamounts including the specification that seamounts are "conical in form". Thus features having a width/length ratio of <0.5 are defined here as ridges (Supplementary Table 15). Ridges are generally larger (mean size of 2570 km^2 versus 810 km^2 for seamounts) and less steep-sided than seamounts. Escarpments characterise 46.1% of ridge flanks compared with 63.4% of seamounts and guyots globally (see Supplementary Table 12).

The 3796 ridges mapped in this study occur in all oceans and cover an area of 9,770,720 km^2. The sum of seamount and ridge area in our study (8,796,150 km^2 + 9,770,720 km^2 = 18,566,870 km^2) is comparable to the estimate of 17.2 million km^2 seamount area reported by Yesson et al. (2011), which suggests that our ridge category overlaps with area mapped as seamounts by Yesson et al. (2011). Thus, recognition of ridges as a separate geomorphic feature category has the effect of dramatically reducing the apparent number of seamounts in the global ocean.

8. Conclusions

The production of a new global seafloor geomorphic features map (GSFM) has provided the basis for the first quantitative assessment of ocean geomorphology. Estimations of area and enumeration at a global scale of many features has been carried out for the first time which has provided the basis to quantify geomorphic differences between active and passive margins as well as differences between eight major ocean regions. Many applications of the GSFM are possible and three have

Table 9
Selected statistics of submarine canyons.

Ocean	All canyons (No.)	All canyons mean area (km²)	All canyons mean length (km)	Slope that is canyon area (%)	Shelf-incising mean incision depth (m)	Self-incising average size (km²)	Shelf-incising mean length (km)	Blind canyon average size (km²)	Blind canyon mean length (km)
Arctic Ocean	404	890	58.9	16.1	1619	2160	99.6	600	49.7
Indian Ocean	1590	480	44.4	11.2	1401	754	56.0	415	41.7
Mediterranean and Black Seas	817	200	26.6	13.8	1093	307	33.1	134	22.7
North Atlantic	1548	480	42.0	10.4	1565	997	63.8	355	36.8
North Pacific	2085	390	38.8	10.2	1424	751	56.9	281	33.2
South Atlantic	453	640	49.2	8.9	1349	894	66.0	594	46.0
South Pacific	2009	350	35.7	10.2	1346	584	46.6	292	33.2
Southern Ocean	571	1000	59.4	15.1	1575	1104	63.7	949	57.5
All oceans	9477	460	41.1	11.2	1395	777	54.8	375	37.3

Table 10
Selected statistics of seamounts and guyots in different ocean regions.

Ocean	Seamount area (km²)	Seamount number	Mean seamount size (km²)	Guyot area (km²)	Guyot number	Mean guyot size (km²)
Arctic	5380	16	340	0	0	0
Indian Ocean	966,990	1082	890	67,010	28	2390
Mediterranean and Black Seas	7700	23	330	2800	2	1400
North Atlantic Ocean	509,200	773	660	31,640	8	3960
North Pacific Ocean	3,097,050	3934	790	499,990	119	4200
South Atlantic Ocean	790,690	952	830	133,710	43	3110
South Pacific Ocean	2,330,400	2961	790	187,900	77	2440
Southern Ocean	151,780	246	620	13,870	6	2310
All oceans	7,859,200	9951	790	936,920	283	3310

been explored here in some detail. First, combining the GSFM with a dataset on seafloor spreading rate provides insights into geomorphic expressions of fast versus slow seafloor spreading rates, which appear to correlate with the occurrence of small versus large rift valley segment sizes, respectively. Second, the spatial analysis of submarine canyons, abyssal roughness, abyssal plains and rises demonstrates that significant geomorphic differences occur between polar and non-polar margins that are attributed here to continental glaciations. And third, recognition of seamounts as being a separate category of feature from ridges resulted in our estimates of seamount number and area being much less than the estimates of previous workers who did not distinguish between ridges and seamounts in their classification.

For future work, the GSFM provide the basis for: interpretations of features as being the product of a particular geological process (i.e. process studies); analyses of the geomorphic composition of different areas of the oceans (i.e. spatial analysis); and improved methods for interpretation and mapping of features (i.e. seafloor feature mapping studies). Since the GSFM is essentially an interpretation of available bathymetric data based on current knowledge of seafloor processes and geology, it is best viewed as a work in progress. As new, higher resolution, bathymetric data become available and as our knowledge of the oceans improves, the GSFM will also change and improve.

Appendix A. Supplementary data

Supplementary data to this article can be found online at http://dx. doi.org/10.1016/j.margeo.2014.01.011.

References

Agapova, G.V., Budanova, L.Y., Zenkevich, N.L., Larina, N.I., Litvin, V.M., Marova, N.A., Rudenko, M.V., Turko, N.N., 1979. Geomorphology of the Ocean Floor, Geofizika okeana. Geofizika okeanskogo dna, Neprochnov, Izd. Nauka, Moscow, pp. 150–205.

Anderson, J.B., 1999. Antarctic Marine Geology. Cambridge University Press, Cambridge, UK.

Baker, E.T., German, C.R., 2004. On the global distribution of hydrothermal vent fields. In: German, C.R., Lin, J., Parson, L.M. (Eds.), Mid-Ocean Ridges: Hydrothermal Interactions between the Lithosphere and Oceans. Geophysical Monograph Series, 148. American Geophysical Union, pp. 245–266.

Beaulieu, S.E., 2013. InterRidge Global Database of Active Submarine Hydrothermal Vent Fields: prepared for InterRidge, Version 3.2. http://vents-data.interridge.org.

Becker, J.J., Sandwell, D.T., Smith, W.H.F., Braud, J., Binder, B., Depner, J., Fabre, D., Factor, J., Ingalls, S., Kim, S.H., Ladner, R., Marks, K., Nelson, S., Pharaoh, A., Trimmer, R., Von Rosenberg, J., Wallace, G., Weatherall, P., 2009. Global bathymetry and elevation data at 30 arc seconds resolution: SRTM30_PLUS. Marine Geodesy 32, 355–371.

Clark, M.R., Watling, L., Smith, C., Rowden, A., Guinotte, J.M., 2011. A global seamount classification to aid the scientific design of marine protected area networks. Ocean and Coastal Management 54, 19–36.

Cooper, A.K., O'Brien, P.E., 2004. Leg 188 synthesis: transitions in the glacial history of the Prydz Bay region, East Antarctica, from ODP drilling. In: Cooper, A.K., O'Brien, P.E., Richter, C. (Eds.), Proceedings of the Ocean Drilling Program, Scientific Results. Ocean Drilling Program, pp. 1–42.

Covault, J.A., 2011. Submarine fans and canyon–channel systems: a review of processes, products, and models. Nature Education Knowledge 3 (10), 4 http://www.nature. com/scitable/knowledge/library/submarine-fans-and-canyon-channel-systems-a-24178428.

Curray, J.R., Emmel, F.J., Moore, D.G., 2002. The Bengal Fan: morphology, geometry, stratigraphy, history and processes. Marine and Petroleum Geology 19, 1191–1223.

Divins, D., 2003. Total Sediment Thickness of the World's Oceans and Marginal Seas. NOAA National Geophysical Data Center.

Dowdeswell, J.A., Cofaigh, C., Noormets, R., Larter, R.D., Hillenbrand, C.D., Benetti, S., Evans, J., Pudsey, C.J., 2008. A major trough-mouth fan on the continental margin of the Bellingshausen Sea, West Antarctica: the Belgica Fan. Marine Geology 252, 129–140.

EMODNet, 2013. European Marine Observation and Data Network, Digital Terrain Model data derived from the EMODnet Hydrography portal. http://www.emodnet-hydrography.eu.

Etnoyer, P.J., Wood, J., Shirley, T.C., 2010. How large is the seamount biome? Oceanography 23, 206–209.

Gardner, J.V., Armstrong, A.A., 2011. The Mariana Trench: a new view based on multibeam echosounding. abstract #OS13B-1517 American Geophysical Union, Fall Meeting 2011 (San Francisco).

Gille, S.T., Metzger, E.J., Tokmakian, R., 2004. Seafloor topography and ocean circulation. Oceanography 17, 47–54.

Gualtieri, L., Vartanyan, S., Brigham-Grette, J., Anderson, P.M., 2003. Pleistocene raised marine deposits on Wrangel Island, northeast Siberia and implications for the presence of an East Siberian ice sheet. Quaternary Research 59, 399–410.

Hambrey, M.J., 1994. Glacial Environments. UCL Press, London.

Harris, P.T., 2011. Benthic environments of the Lord Howe Rise submarine plateau: introduction to the special volume. Deep Sea Research Part II 58, 883–888.

Harris, P.T., Baker, E.K. (Eds.), 2012. Seafloor Geomorphology as Benthic Habitat: GeoHab Atlas of Seafloor Geomorphic Features And Benthic Habitats. Elsevier, Amsterdam, p. 947.

Harris, P.T., Whiteway, T., 2011. Global distribution of large submarine canyons: geomorphic differences between active and passive continental margins. Marine Geology 285, 69–86.

Harris, P.T., Heap, A., Passlow, V., Hughes, M., Daniell, J., Hemer, M., Anderson, O., 2005. Tidally-incised valleys on tropical carbonate shelves: an example from the northern Great Barrier Reef, Australia. Marine Geology 220, 181–204.

Heap, A., Harris, P.T., 2008. Geomorphology of the Australian margin and adjacent sea floor. Australian Journal of Earth Sciences 55, 555–584.

Heezen, B.C., Tharp, M., 1977. World Ocean Floor Panorama, New York, pp. In full color, painted by H. Berann, Mercator Projection, scale 1:23,230,300, 1168 × 1930 mm.

Hein, J.R., Conrad, T.A., Staudigel, H., 2010. Seamount mineral deposits — a source of rare metals for high-technology industries. Oceanography 23, 184–189.

IHO, 1953. Limits of Oceans and Seas. International Hydrographic Organisation, Special Publication No 23, Monégasque — Monte-Carlo.

IHO, 2008. Standardization of Undersea Feature Names: Guidelines Proposal form Terminology, 4th ed. International Hydrographic Organisation and Intergovernmental Oceanographic Commission, Monaco.

IHO-IOC, 2012. GEBCO Gazetteer of Undersea Feature Names, October 2012 version.

Jakobsson, M., Macnab, R., Mayer, L., Anderson, R., Edwards, M., Hatzky, J., Schenke, H.W., Johnson, P., 2008. An improved bathymetric portrayal of the Arctic Ocean: implications for ocean modeling and geological, geophysical and oceanographic analyses. Geophysical Research Letters. http://dx.doi.org/10.1029/2008gl033520.

Jenness, J., Brost, B., Beier, P., 2012. Land Facet Corridor Designer: Extension for ArcGIS. Jenness Enterprises (Available at: http://www.jennessent.com/arcgis/land_facets.htm).

Kennett, J., 1982. Marine Geology. Prentice-Hall, Englewood Cliffs, N.J.

Kitchingman, A., Lai, S., 2004. Inferences on potential seamount locations from mid-resolution bathymetric data. In: Morato, T., Pauly, D. (Eds.), FCRR Seamounts: Biodiversity and Fisheries. Fisheries Centre Research Reports. University of British Columbia, Vancouver, BC, pp. 7–12.

Macdonald, K.C., 2001. Mid-ocean ridge tectonics, volcanism and geomorphology. Encyclopedia of Ocean SciencesElsevier 1798–1813.

Mitchell, N.C., 2001. The transition from circular to stellate forms of submarine volcanoes. Journal of Geophysical Research 106, 1987–2003.

Müller, R.D., Roest, W.R., Royer, J.Y., Gahagan, L.M., Sclater, J.G., 1997. Digital isochrons of the world's ocean floor. Journal of Geophysical Research 102, 3211–3214.

Niessen, F., Hong, J.K., Hegewald, A., Matthiessen, J., Stein, R., Kim, H., Kim, S., Jensen, L., Jokat, W., Nam, S.-I., Kang, S.-H., 2013. Repeated Pleistocene glaciation of the East Siberian continental margin. Nature Geoscience 6, 842–846.

Normark, W.R., Carlson, P.R., 2003. Giant submarine canyons: is size any clue to their importance in the rock record? Geological Society of America Special Papers 370, 175–190.

Shepard, F.P., 1963. Submarine Geology. Harper & Row, New York.

Smith, W.H., Sandwell, D.T., 1997. Global sea floor topography from satellite altimetry and ship depth soundings. Sci. Mag. 277, 1956–1962.

Wessel, P., 2001. Global distribution of seamounts inferred from gridded Geosat/ERS-1 altimetry. Journal of Geophysical Research 106, 19431–19441.

Whiteway, T., 2009. Australian Bathymetry and Topography Grid. Record 2009/21Geosci-Geoscience Australia, Canberra.

WRI, 2011. World Resources Institute, Reefs at Risk Revisited. www.wri.org/reef.

Wright, J., Rothery, D.A., 1998. The Ocean Basins: Their Structure and Evolution, 2nd ed. Elsevier.

Yesson, C., Clark, M.R., Taylor, M.L., Rogers, A.D., 2011. The global distribution of seamounts based on 30 arc seconds bathymetry data. Deep Sea Research Part I: Oceanographic Research Papers 58, 442–453.